Quantum Chromo Dynamics (QCD) in hadronic collisions

Theory and Experiments

Antonio Sidoti[1]

[1]Istituto Nazionale Fisica Nucleare
Sezione di Bologna
antonio.sidoti@bo.infn.it

Hasco Summer School, July 2015

If lectures too easy, too hard, too boring,....

PLEASE REACT !

YOU ARE FREE TO ASK QUESTIONS DURING THE LECTURES.

I WILL TRY GIVE BEST ANSWERS (OR POSTPONE THEM)

YOU CAN ALWAYS ASK ME THIS WEEK OR ASK BY EMAIL

There is plenty of material in these lectures (probably too much)

It will be impossible to cover all of the topics

→ Try to give a feeling of QCD you need at hadron colliders

What these lectures won't cover:

- Historical introduction to QCD (quark static model, $SU(3)_F$)
- Lattice QCD
- Hadron spectroscopy (no pentaquarks!)
- Quark-Gluon plasma (QGP)

Some references to:

- QCD in e^+e^- collisions
- Deep Inelastic Scattering (DIS)

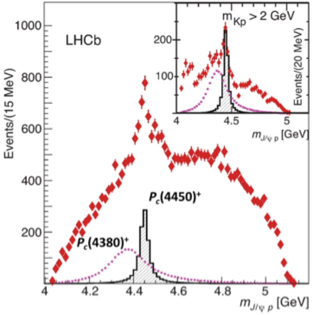

From LHCb experiment arXiv1507.03414

Major milestones in QCD

1950 Quantum Electrodynamics (QED) is the quantum field theory (QFD) describing electromagnetic interactions

1960 Explosion of baryon and mesons zoo, static model of quarks. S-Matrix theory (No QFD for strong interactions!)

Experimental evidence of partons

1970 Standard Model and Quantum Chromodynamics (QCD): The QFD for strong interactions (Renormalizability of gauge theories)

1980 Experimental evidence of gluons

Table of Contents

Table of Contents

Physics Processes at LHC (ATLAS) (Run1: 7 and 8 TeV)

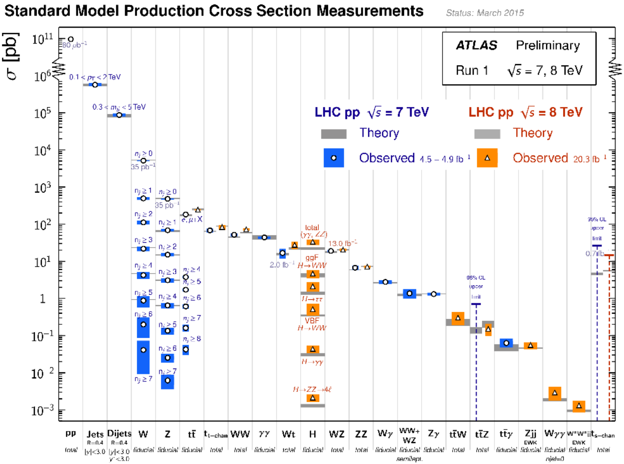

QCD is the toolbox for discoveries at the LHC

Searches for Physics Beyond Standard Model

Searches for dijet mass resonances

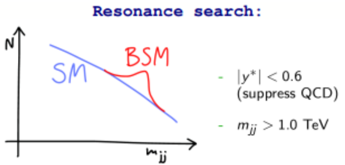

- "SM background" is mainly from QCD
- Not only Breit-Wigner but also "dips" due to interference effects
- Shape and normalization from fit to sidebands (etc...)

Angular searches for BSM

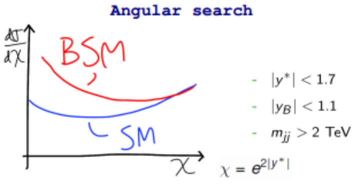

- $\chi = \exp\{2|y^\star|\}$
- Shape and normalization from fit to data

Although background contribution is data driven a precise prediction of QCD is fundamental to assess physics BSM (*cf* lecture on Susy and Exotics).

Table of Contents

QCD

Quantum Chromodynamics is:
one of the pillars of the Standard Model.
the theory of quarks, gluon and their interactions (Strong interaction):
central to modern colliders (LHC)
SM → gauge theory based on the $SU_C(3) \otimes SU(2) \otimes U(1)_Y$ group
$SU_C(3)$ is the color group for QCD
$SU_C(3)$ is an exact symmetry
$SU(2) \otimes U(1)_Y$ is the *electroweak* symmetry group → (*Standard Model* and *Higgs* lectures)

QCD and Hadrons

Up to few weeks ago (and still TBC !) quarks can be combined in color-less mesons and baryons (singlets of $SU_C(3)$)

Mesons (bosons, e.g. pion ...)

$$\sum_i \psi_i^* \psi_i \rightarrow \sum_{ijk} U_{ij}^* U_{ik} \psi_j \psi_k = \sum_k \psi_k^* \psi_k$$

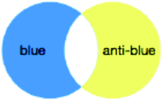

Baryons (fermions, e.g. proton, neutrons ...)

$$\sum_{ijk} \epsilon_{ijk} \psi_i \psi_j \psi_k \rightarrow \sum_{ii'jj'kk'} \epsilon_{ijk} U_{ii'} U_{jj'} U_{kk'} \psi_{i'} \psi_{j'} \psi_{k'} = \sum_{i'j'k'} \epsilon_{i'j'k'} \det(U) \psi_{i'} \psi_{j'} \psi_{k'}$$

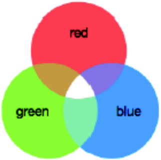

QED vs QCD

Gauge group	
U(1)	SU(3)
Charge	
electric charge e	color e_s (three colors)
Mediator	
1 photon A	8 gluons g
Lagrangian	
$\mathcal{L} = -\frac{1}{4}F^{\mu\nu}F_{\mu\nu} + \sum_\psi \bar{\psi}(i\not{D} - m_\psi)\psi$.	$\mathcal{L} = -\frac{1}{4}\sum_{A=1}^{8} F^{A\mu\nu}F^A_{\mu\nu} +$ $+ \sum_{j=1}^{n_f} \bar{q}_j(i\not{D} - m_j)q_j$
$F_{\mu\nu} = \partial_\mu A_\nu - \partial_\nu A_\mu$	$F^A_{\mu\nu} = \partial_\mu g^A_\nu - \partial_\nu g^A_\mu - e_s C_{ABC} g^B_\mu g^C_\nu$
$\not{D} = D_\mu \gamma^\mu$	
$D_\mu = \partial_\mu - ieA_\mu Q$.	$D_\mu = \partial_\mu - ie_s \mathbf{g}_\mu$ $\mathbf{g}_\mu = \sum_\mathbf{A} \mathbf{T}^\mathbf{A} \mathbf{g}^\mathbf{A}_\mu$
$\alpha_{QED} = \frac{e^2}{4\pi}$	$\alpha_s = \frac{e_s^2}{4\pi}$

QCD Lagrangian

$$\mathcal{L} = -\frac{1}{4}\sum_{A=1}^{8} F^{A\mu\nu}F^{A}_{\mu\nu} + \sum_{j=1}^{n_f} \bar{q}_j(i\not{D} - m_j)q_j$$

$$F^A_{\mu\nu} = \partial_\mu g^A_\nu - \partial_\nu g^A_\mu - e_s C_{ABC} g^B_\mu g^C_\nu$$

$$D_\mu = \partial_\mu - i e_s g_\mu$$

$$g_\mu = \sum_A T^A g^A_\mu$$

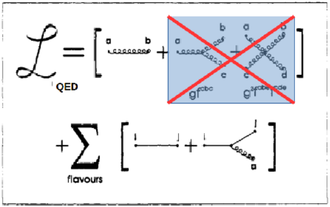

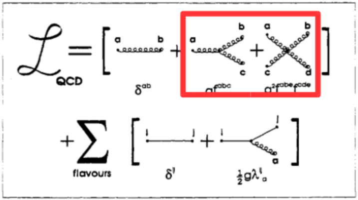

Feynman Graphs (I)

QED

$$\to \left(\frac{i}{\not p - m + i\varepsilon}\right)_{\beta\alpha}$$

fermion propagator

$$\to \frac{-i\eta_{\mu\nu}}{p^2 + i\varepsilon}$$

Photon propagator

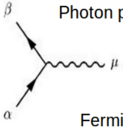

$$\to -ie\gamma^{\mu}_{\beta\alpha}(2\pi)^4\delta^{(4)}(p_1+p_2+p_3).$$

Fermion-photon vertex

QCD

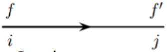

$$= \frac{i\delta^i_j\delta^f_{f'}}{\not p - m_f + i0}.$$

Quark propagator

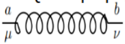

$$= \frac{-i\delta^{ab}}{k^2+i0}\left(g^{\mu\nu} + (\xi - 1)\frac{k^\mu k^\nu}{k^2+i0}\right).$$

Gluon propagator

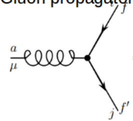

$$= -ig\gamma^\mu \times \delta^{f'}_f \times (t^a)^j_i.$$

Quark-gluon vertex

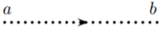

$$= \frac{i\delta^{ab}}{k^2+i0}.$$

Ghost propagator (gauge fixing terms)

Feynman Graphs (II)

QCD only: triple and quartic gluon vertices:
From non commutative of SU(3) matrices:

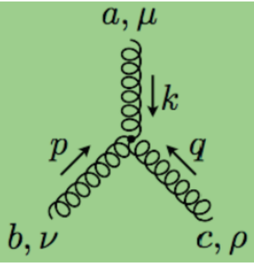

$$= g_s f^{abc}\left[g^{\mu\nu}(k-p)^\rho + g^{\nu\rho}(p-q)^\mu + g^{\rho\mu}(q-k)^\nu\right]$$

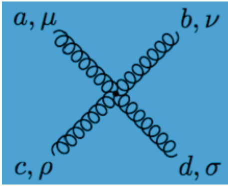

$$= -ig_s^2\left[f^{abe}f^{cde}\left(g^{\mu\rho}g^{\nu\sigma}-g^{\mu\sigma}g^{\nu\rho}\right) + f^{ace}f^{bde}\left(g^{\mu\nu}g^{\rho\sigma}-g^{\mu\sigma}g^{\nu\rho}\right) + f^{ade}f^{bce}\left(g^{\mu\nu}g^{\rho\sigma}-g^{\mu\rho}g^{\nu\sigma}\right)\right]$$

Example: quark gluon vertex

What $\bar{\psi}_b(-ig_S t^A_{ba}\gamma_\mu)\psi_a$ means?

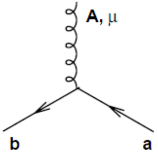

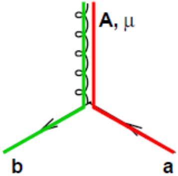

$$\underbrace{\begin{pmatrix} \color{red}{0} & \color{green}{1} & \color{blue}{0} \end{pmatrix}}_{\bar{\psi}_b} \underbrace{\begin{pmatrix} 0 & 1 & 0 \\ 1 & 0 & 0 \\ 0 & 0 & 0 \end{pmatrix}}_{t^1_{ab}} \underbrace{\begin{pmatrix} \color{red}{1} \\ \color{green}{0} \\ \color{blue}{0} \end{pmatrix}}_{\psi_a} + \begin{pmatrix} \color{red}{0} & \color{green}{1} & \color{blue}{0} \end{pmatrix} \underbrace{\begin{pmatrix} 0 & -i & 0 \\ i & 0 & 0 \\ 0 & 0 & 0 \end{pmatrix}}_{t^2_{ab}} \begin{pmatrix} \color{red}{1} \\ \color{green}{0} \\ \color{blue}{0} \end{pmatrix} + \dots$$

gluon emission change the color of the quark

Some Useful Formulas

$$\mathrm{Tr}(t^A t^B) = T_R \delta^{AB}\,, \quad T_R = \tfrac{1}{2}$$

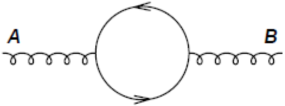

$$\sum_A t^A_{ab} t^A_{bc} = C_F \delta_{ac}\,, \quad C_F = \frac{N_c^2 - 1}{2N_c} = \frac{4}{3}$$

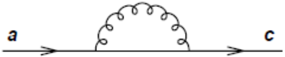

$$\sum_{C,D} f^{ACD} f^{BCD} = C_A \delta^{AB}\,, \quad C_A = N_c = 3$$

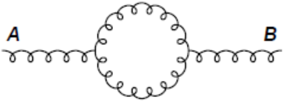

$$t^A_{ab} t^A_{cd} = \frac{1}{2}\delta_{bc}\delta_{ad} - \frac{1}{2N_c}\delta_{ab}\delta_{cd} \quad \text{(Fierz)}$$

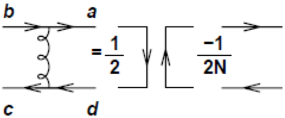

$N_c \equiv$ number of colours $= 3$ for QCD

from G. Salam lectures at Maria Laach

Vacuum polarization

In QED electron and positron *virtual* clouds effectively screen the electric charge:

- Probe close ⇒ Large effective charge
- Probe far ⇒ small effective charge

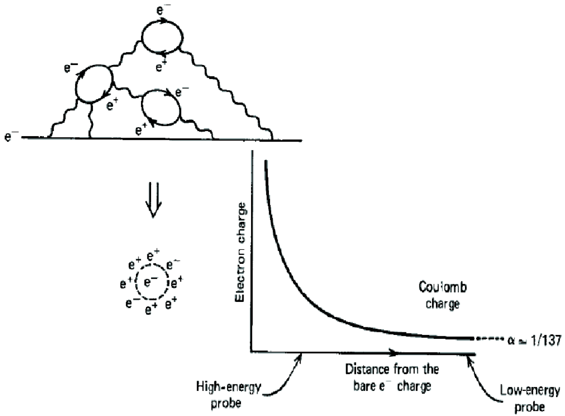

Vacuum polarization

In QCD Together with quark-antiquark *virtual* clouds there are also pure gluon loops:

- Probe close ⇒ small effective charge (Asymptotic Freedom)
- Probe far ⇒ large (infinite) effective charge (Confinement)

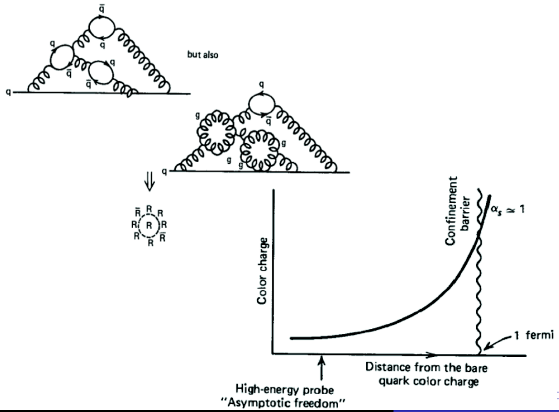

Perturbation theory

If $\alpha_s \ll 1$ expansion is α_s order is possible:

$$\mathcal{O} = \alpha_s + \underbrace{\alpha_s^2}_{small} + \underbrace{\alpha_s^3}_{smaller} + \underbrace{\ldots}_{negligible}$$
$$= LO + NLO + NNLO + \ldots$$

However if α_s is large (momentum $\sim \Lambda_{QCD}$) power series is not convergent $\Rightarrow$ cannot use perturbative approach. pQCD doesn't hold anymore.

$\Rightarrow$ need alternative approaches (*e.g.* Lattice QCD, phenomenological approaches, ...)

Consequences

While we can observe electrons, muons in nature, quarks and gluons cannot be observed as free charges (except top quark).

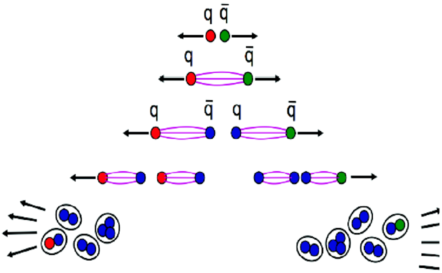

- a quark-antiquark pair is created in the final state
- color lines stretches so much that new $q\bar{q}$ pairs pop-out from vacuum (typical energies $\sim Q$)
- process is repeated until $Q \sim \Lambda_{QCD} \sim \mathcal{O}(\sim 100 MeV)$
- Hadronization occurs to form *physical* particles (mesons, baryons) $\Rightarrow$ this is a non-perturbative process

Renormalization

UV Singularities

Let's consider gluon-quark vertex.

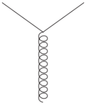

Tree-level (Born-level or Leading Order (LO) graph)

Renormalization

UV Singularities

Let's consider gluon-quark vertex.

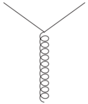

Tree-level (Born-level or Leading Order (LO) graph)

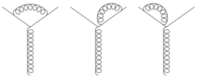

Need to add gluon propagator loops....

Renormalization

UV Singularities

Let's consider gluon-quark vertex.

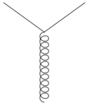

Tree-level (Born-level or Leading Order (LO) graph)

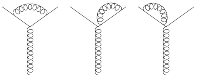

Need to add gluon propagator loops....

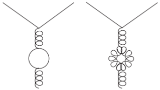

and vacuum polarization graphs.

Renormalization

UV Singularities

Let's consider gluon-quark vertex.

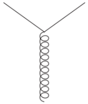

Tree-level (Born-level or Leading Order (LO) graph)

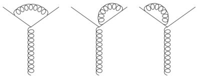

Need to add gluon propagator loops....

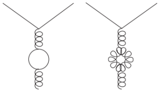

and vacuum polarization graphs.

These are only second order graphs (Next to Leading Order (NLO)). Also present third (NNLO) *etc.*

Each loop $\rightarrow \int_{k=0}^{+\infty} d^4k$

Each additional vertex $\rightarrow (ig_s)$ (that is $\sqrt{\alpha_s} \rightarrow |\mathcal{M}|^2 \rightarrow \alpha_s$)

Quark Energy One Loop

As an example let's calculate quark propagator at one loop: Use Feynman gauge ($\xi = 1$):

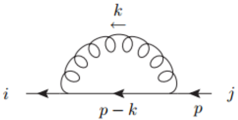

$$
\delta_{ij}\frac{i}{\not p - m} \rightarrow
$$

$$
\int \frac{d^4k}{(2\pi)^4}(ig_s)\gamma_\mu T^a_{ik}\delta_{kl}\frac{i}{\not p - \not k - m + i\epsilon}(ig_s)\gamma_\nu T^b_{lj}\delta_{ab}\frac{(-i)g^{\mu\nu}}{k^2 + i\epsilon}
$$

$$
= C_F\frac{g_s^2}{i}\int\frac{d^4k}{(2\pi)^4}\frac{\gamma_\mu(\not p - \not k + m)\gamma^\mu}{k^2((p-k)^2 - m^2)}
$$

$$
\text{where } C_F = \frac{N_c^2 - 1}{2N_c} \text{ for } SU(N_c) \text{ and} (T^aT^a)_{ij} = \delta_{ij}C_F
$$

$$
\sim \int d^4k\frac{\not k}{k^2k^2} \sim \int k^3dk\frac{k}{k^4} \sim \int dk
$$

that is divergent when integration bound goes to ∞. $\Rightarrow$ Ultraviolet (UV) divergence

Regularization

[shrink=10] To handle UV divergences need a regularization procedure. Two strategies:

- *cu-off* regularization. All calculations are carried out up to a finite momentum K. Limit to $+\infty$ is performed later.
- *Dimensional* regularization. Note that integral is divergent in 4D but convergent in 2D. $\Rightarrow$ expand in continuous $\epsilon = (4 - D)/2$. Appearance of single poles for $\epsilon \to 0$. This is the one normally used in QCD

Generic $N-$loop amplitude I_N:

$$I_N = \sum_{n=0}^{N} \left(\frac{\alpha_s}{4\pi}\right)^2 \frac{C_n}{\epsilon^n} + \mathcal{O}(\epsilon)$$

Renormalization

Pragmatic strategy to deal with UV divergencies:

- Start from original Lagrangian $\mathcal{L}$
- For each order in α_s identify divergent diagrams.
- Add counterterms in the original Lagrangian such to cancel divergent diagrams.

$$\begin{aligned}\mathcal{L}_{renorm} &= \mathcal{L} + \mathcal{L}^{(1)}_{counter} + \mathcal{L}^{(2)}_{counter} + \dots \\ &= \mathcal{L} + \mathcal{L}_{counter}\end{aligned}$$

- Luckily $\mathcal{L}_{counter}$ can be expressed as $\mathcal{L}$ by replacing (rescaling, renormalizing) $m \to m_0 = Z_m m$, $\psi \to \psi_0 Z_\psi^{1/2}$, $\alpha_s \to \alpha_{s0}\mu^\epsilon$, etc.
- $\mathcal{L}_{counter}$ is still gauge invariant provided all this Z_X factors depend on single renormalization Z_g factor such that $Z_g = \frac{\alpha_{s0}}{\alpha_s \mu_R^\epsilon}$ (Becchi-Rouet-Stora Theorem)

We have now a divergent free Lagrangian that is now dependent on μ_R (dimension of a mass). μ_R is called Renormalization scale.

Different criteria to cancel out divergent diagrams: *renormalization schemes*.
Most common are MS, $\overline{\rm MS}$, *on mass-shell* scheme, etc.

Two arbitrary choices:

- choice of μ_R renormalization scheme
- choice of renormalization scheme

Note that physical observables are independent on choice of μ_R and scheme
But truncated expansion are NOT!

A generic observable $R\left(Q^2/\mu^2, \alpha\right)$ cannot depend on μ_R.
Any change in μ_R is compensated by a change in α_s

$$\mu \frac{d}{d\mu^2} R\left(Q^2/\mu^2, \alpha\right) = \left(\mu^2 \frac{\partial}{\partial \mu^2} + \mu^2 \frac{\partial \alpha}{\partial \mu^2} \frac{\partial}{\partial \alpha}\right) R = 0$$

$$\text{with} t = \log\left(\frac{Q^2}{\mu^2}\right) \quad \text{and} \quad \beta(\alpha) = \mu^2 \frac{\partial \alpha}{\partial \mu^2}$$

$$\left(\frac{\partial}{\partial t} + \beta(\alpha) \frac{\partial}{\partial \alpha}\right) R = 0$$

$$\frac{\partial \alpha}{\partial t} = \beta(\alpha) \quad \text{or} \quad Q^2 \frac{\partial \alpha}{\partial Q^2} \beta(\alpha)$$

These are called Renormalization Group Equation (RGE).

Running Coupling Constant

- Beta function of RGE specifies running of $\alpha_s(Q^2)$ with: $\frac{\partial \alpha}{\partial t} = \beta(\alpha)$
- pert expansion of beta function: $\beta(\alpha_s) = -b\alpha_s^2\left(1 + b'\alpha_s + b''\alpha_s^2 + ...\right)$
- 1-loop beta-function sums up leading $\log\frac{Q^2}{\mu^2}$

1–loop

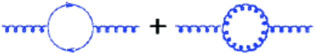

$$b = \frac{33 - 2n_f}{12\pi}$$

2–loops

$$b' = \frac{153 - 19n_f}{2\pi(33 - 2n_f)}$$

3–loops

$$b'' = \frac{77139 - 15099n_f + 325n_f^2}{288\pi^2(33 - 2n_f)}$$

scheme dependence enters at *b*"

H. Jung lectures: (QCD and collider physics) Desy Lectures

α running in QCD

Limiting to 1-loop:

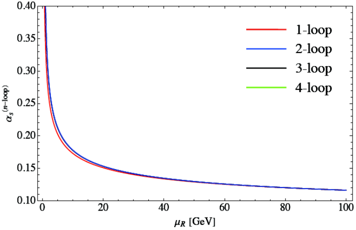

$$\alpha_s = \frac{\alpha_s(\mu^2)}{1 + \frac{\alpha_s(\mu^2)}{12\pi}(33 - 2n_f)\log\frac{Q^2}{\mu^2}}$$

Defining

$$\Lambda^2_{QCD} = \mu^2 \exp\left(\frac{-12\pi}{(33-2n_F)\alpha_s(\mu^2)}\right) \simeq \mathcal{O}(200)\text{MeV}$$

Running coupling

$$\alpha_s = \frac{12\pi}{(33-2n_f)\log\frac{Q^2}{\Lambda^2_{QCD}}}$$

2004 Nobel prize: Gross, Politzer and Wilczek

α running in QCD

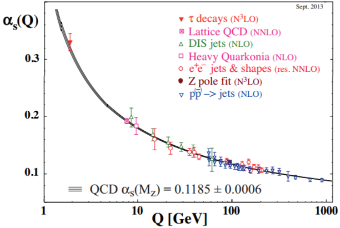

from Particle Data Group
from Particle Data Group
Note that also in QED α_{em} is running but with different sign of β=function (Remember $\alpha_{em}(0) = 1/137$):

$$\alpha_{em}(Q^2) = \frac{\alpha_{em}(\mu^2)}{1 + \beta_0 \alpha(\mu^2) \ln(Q^2/\mu^2)}$$

$$\text{with} \quad \beta_0 = -\frac{1}{3\pi}$$

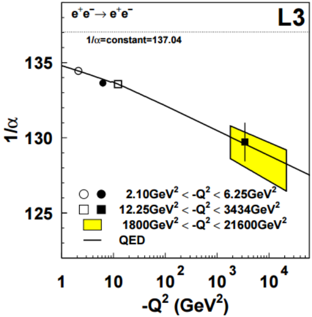

from L3 hep-ex/0507078

μ_R dependency

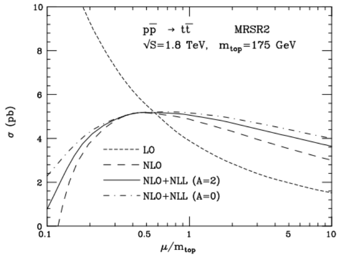

$t\bar{t}$ cross section at $\sqrt{s} = 1.8$ TeV
$\sigma_{t\bar{t},LO} \in [5.5, 2.8]$ for $m_t/2 < \mu_R < 2mt$
$\sigma_{t\bar{t},NLO} \in [4.8, 5.1]$ for $m_t/2 < \mu_R < 2mt$

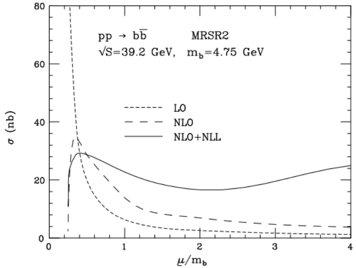

$p\bar{p} \to b\bar{b}$ hadroproduction cross section at $\sqrt{s} = 39.2$ GeV $\sigma_{b\bar{b},LO} \in [\sim 8, \sim 24]$ for $m_b/2 < \mu_R < 2m_b$
$\sigma_{b\bar{b},NLO} \in [\sim 16, \sim 28]$ for $m_b/2 < \mu_R < 2m_b$

from Bonciani et al. hep-ph/9801375

Physics observables are not dependent on μ_R but truncated calculations do!
Improves going from LO to NLO (an NNLO!)

Infrared (IR) Divergencies

Consider process $e^+e^- \to q\bar{q}g$ through photon annihilation:

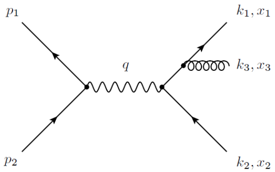

Kinematics in the center-of-mass frame:

$$\begin{aligned} q &= p_1 + p_2 \\ &= k_1 + k_2 + k_3 \\ q^2 &= q^\mu q_\mu = s \\ E_i &= k_i^0 \\ x_i &= \frac{E_i}{\sqrt{s}/2} \text{ energy fraction} \\ &= \frac{2q \cdot k_i}{s} \end{aligned}$$

Note that $x_1 + x_2 + x_3 = 2 \to$ only two x_i are independent. After some calculation the cross section can be expressed as:

$$\frac{d^2\sigma}{dx_1 dx_2} = \sigma_0 \frac{2\alpha_s}{3\pi} \frac{x_1^2 + x_2^2}{(1-x_1)(1-x_2)}$$

where $\sigma_0 = \sigma(e^+e^- \to \text{hadrons}) = \frac{3\pi}{\alpha_s^2} \sum e_i^2$.

Infrared (IR) Divergences

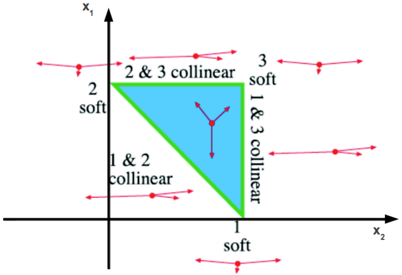

Divergences on the boundaries of kinetically allowed region. Origin is in the quark propagator

$$\sim \frac{1}{(k_1+k_2)^2} \to \frac{1}{2E_1E_3(1-\cos\theta_{31})}$$

- colinear divergence $\theta_{13} \to 0$
- soft divergence $E_3 \to 0$

The $e^+e^- \to qqg$ cross section becomes logarithmic divergent:

$$\frac{d\sigma}{dE_3 d\cos\theta_{31}} = \sigma_0 \frac{2\alpha_s}{3\pi} \frac{f(E_3,\theta_{31})}{E_3(1-\cos\theta_{31})}$$

Now remember Heisemberg uncertainty principle $\Delta E \Delta t \sim 1$ IR divergences are connected to long time scales compared to $q\bar{q}$ production.

Observables infrared and collinear (IRC) safe

How to deal with IR divergences?:

- Resummation to all order (similar to UV) (In some case even regularization is not needed). *e.g.* gluon multiplicity
- Calculation (and measurement) of IRC safe observables.

Important

For an observable's distribution to be calculable in (fixed order) perturbation theory, the observable should be infrared-safe, i.e. insensitive to the emission of soft or collinear gluons. In particular if $\vec{p}_i$ is any momentum occurring in its definition, it must be invariant under the branching:

$$\vec{p}_i \rightarrow \vec{p}_j + \vec{p}_k$$

whenever $\vec{p}_j$ and $\vec{p}_k$ are parallel (collinear) or one of them is small (infrared) (*from QCD and Collider Physics (Ellis, Stirling Webber)*)

Example of Observables

- Gluon multiplicity is NOT IRC safe (but can be resummed to all orders)

$$< N_g > \sim \sum_n \frac{1}{(n!)^2} \left(\frac{C_A}{\pi b} \ln \frac{Q}{\Lambda} \right)^n$$
$$\sim \exp \sqrt{\frac{4 C_A}{\pi b} \ln \frac{Q}{\Lambda}} \text{ with } C_A = 3 \text{ and } \Lambda = 220\text{MeV}$$

- Energy of hardest particle **is not IRC safe**
- Energy flow into a cone **is IRC safe** (Sterman-Weinberg jets)

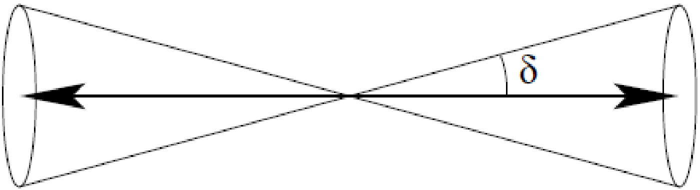

A proton-proton collision

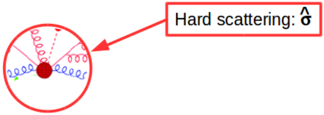

A proton-proton collision

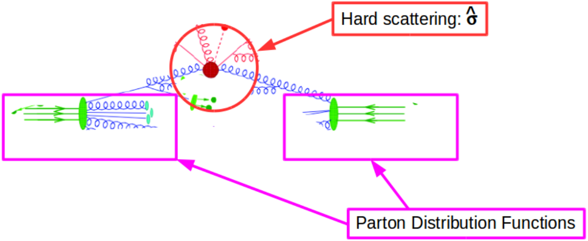

A proton-proton collision

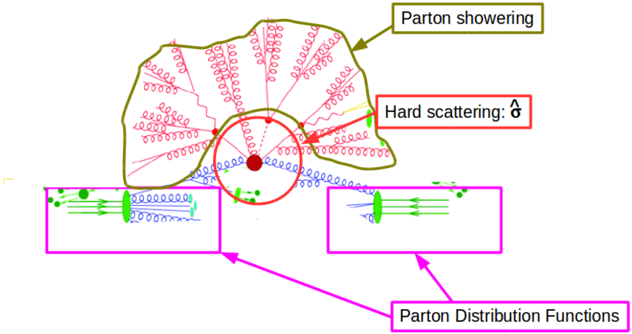

A proton-proton collision

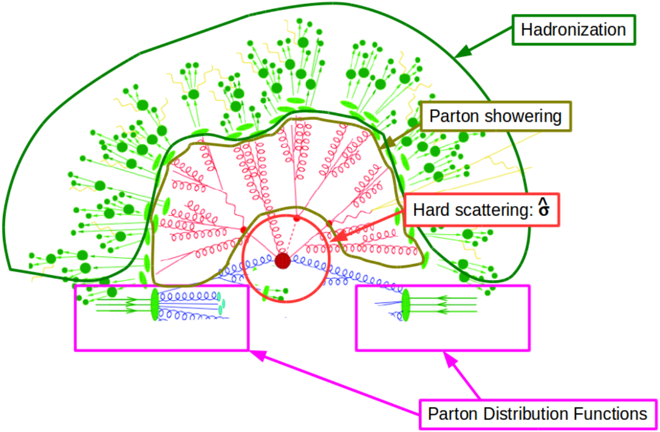

A proton-proton collision

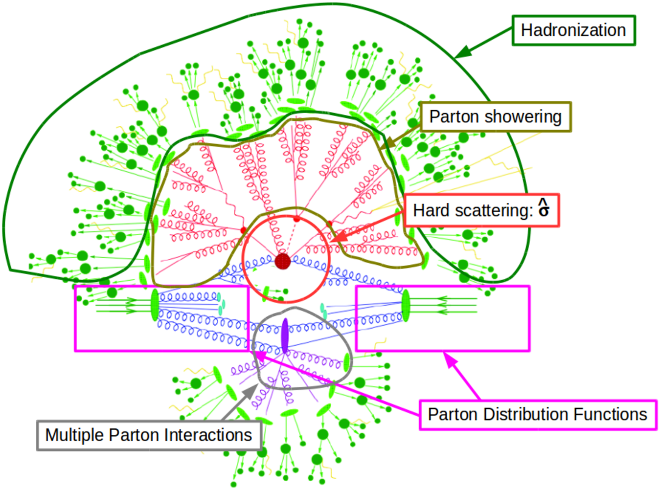

A proton-proton collision

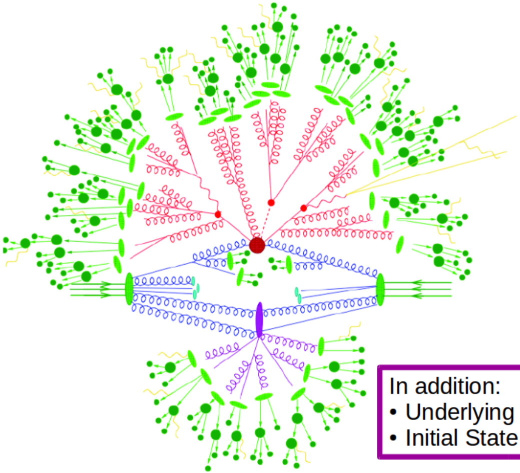

In addition:
- Underlying Event
- Initial State Radiation

MonteCarlo Simulations

It is difficult to underestimate the importance of MonteCarlo (MC) simulations in High Energy Physics!
MC simulations are the bridge between theorist/phenomenologist and experimentalists.

Experimentalists shouldn't use MC as black boxes!

There was a tremendous evolution in MC in the last ~10 years

Some Montecarlo programs

Hard scattering (also called ME) processes simulations available at different orders:

Leading Order (LO):

ALPGEN, COMIX/SHERPA, COMPHEP, HELAC/PHEGAS, MADGRAPH, Sherpa, Wizard

A large variety of physics processes (also BSM) 2 → n final states (n up to 8 for some processes)

n fin. state	2	3	4	5	6	7	8
# diagrams	4	25	220	2485	34300	~500k	10M

Number of diagrams for gg → n gluon scattering

Next to Leading Order (NLO):

NLOJET++, MCFM, VBFNLO, PHOX, POWHEG, MC@NLO

Next to Next to Leading Order (NNLO):

Not general purpose MC, but limited to specific processes pp → $t\bar{t}jj$, pp → $tt\bar{b}\bar{b}$, pp → W/Z+3j, pp → H (FEWZ, FeHiP, HNNLO)

Good description of "hard" processes (large angle emission)

Practical simulation of LO, NLO and NNLO processes

Clearly an interplay between multiplicity of final states and order.
As an example, consider $pp \to Z + N$ jets with $N = 0, 1, 2$.

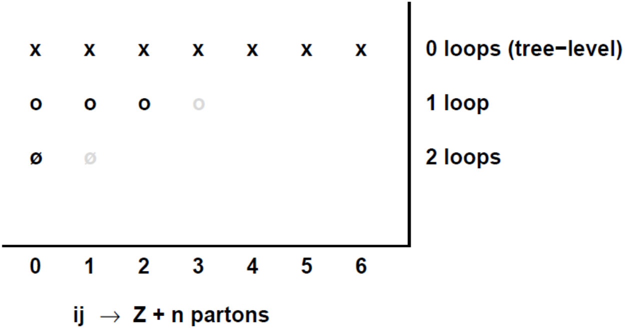

Practical simulation of LO, NLO and NNLO processes

Clearly an interplay between multiplicity of final states and order.
As an example, consider $pp \to Z + N$ jets with $N = 0, 1, 2$.

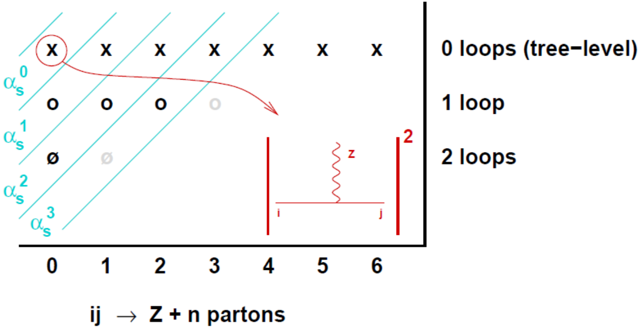

The bottleneck in getting N^pLO predictions is usually either the calculation of the p-loop diagram, or figuring out how to combine (cancel) divergences

Practical simulation of LO, NLO and NNLO processes

Clearly an interplay between multiplicity of final states and order.
As an example, consider $pp \to Z + N$ jets with $N = 0, 1, 2$.

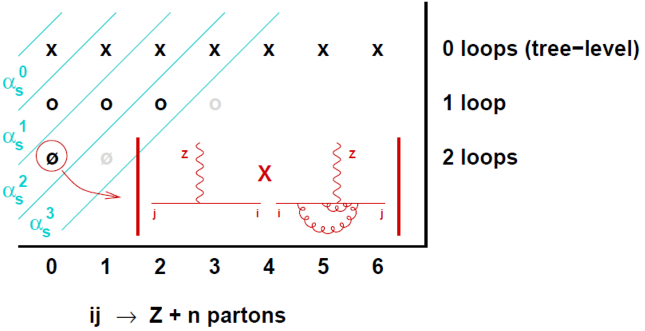

The bottleneck in getting N^{p}LO predictions is usually either the calculation
of the p-loop diagram, or figuring out how to combine (cancel) divergences

Practical simulation of LO, NLO and NNLO processes

Clearly an interplay between multiplicity of final states and order.
As an example, consider $pp \to Z + N$ jets with $N = 0, 1, 2$.

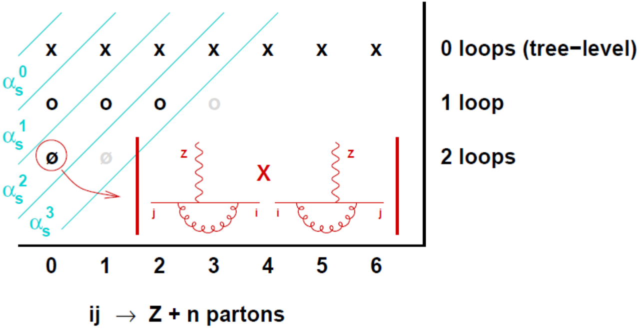

The bottleneck in getting N^{p}LO predictions is usually either the calculation of the p-loop diagram, or figuring out how to combine (cancel) divergences

Practical simulation of LO, NLO and NNLO processes

Clearly an interplay between multiplicity of final states and order.
As an example, consider $pp \to Z + N$ jets with $N = 0, 1, 2$.

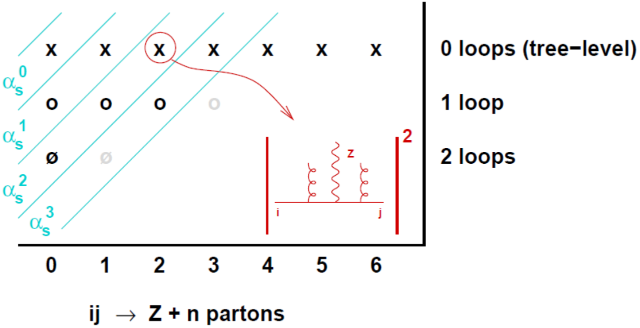

The bottleneck in getting N^{p}LO predictions is usually either the calculation of the p-loop diagram, or figuring out how to combine (cancel) divergences

Practical simulation of LO, NLO and NNLO processes

Clearly an interplay between multiplicity of final states and order.
As an example, consider $pp \to Z + N$ jets with $N = 0, 1, 2$.

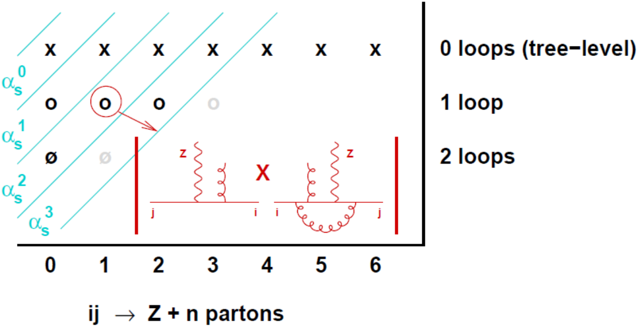

The bottleneck in getting N^{p}LO predictions is usually either the calculation of the p-loop diagram, or figuring out how to combine (cancel) divergences

Practical simulation of LO, NLO and NNLO processes

Clearly an interplay between multiplicity of final states and order.
As an example, consider $pp \to Z + N$ jets with $N = 0, 1, 2$.

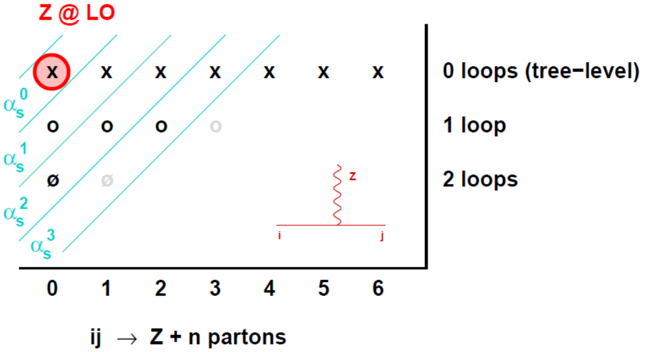

Practical simulation of LO, NLO and NNLO processes

Clearly an interplay between multiplicity of final states and order.
As an example, consider $pp \to Z + N$ jets with $N = 0, 1, 2$.

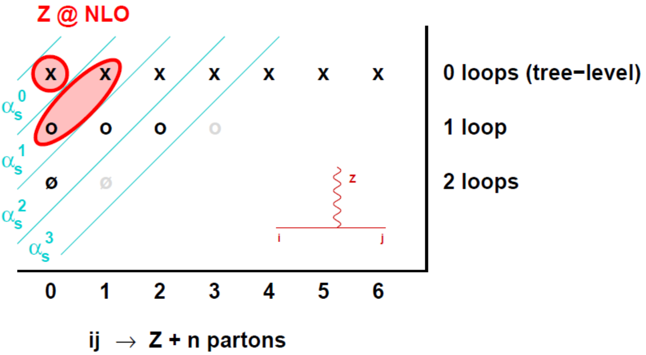

The bottleneck in getting N^{p}LO predictions is usually either the calculation of the p-loop diagram, or figuring out how to combine (cancel) divergences

Practical simulation of LO, NLO and NNLO processes

Clearly an interplay between multiplicity of final states and order.
As an example, consider $pp \to Z + N$ jets with $N = 0, 1, 2$.

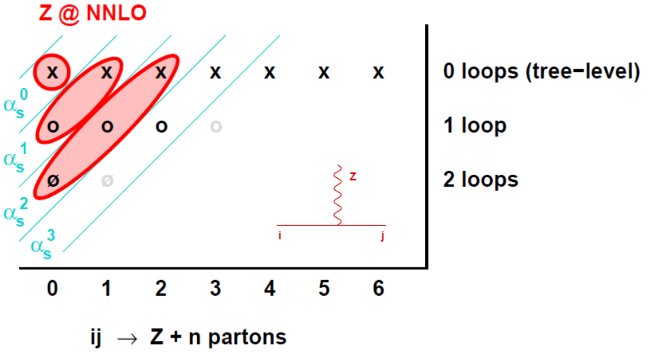

The bottleneck in getting N^{p}LO predictions is usually either the calculation of the p-loop diagram, or figuring out how to combine (cancel) divergences

Practical simulation of LO, NLO and NNLO processes

Clearly an interplay between multiplicity of final states and order.
As an example, consider $pp \to Z + N$ jets with $N = 0, 1, 2$.

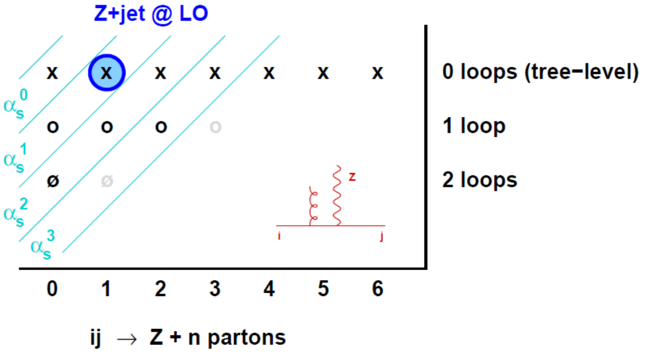

The bottleneck in getting N^pLO predictions is usually either the calculation of the p-loop diagram, or figuring out how to combine (cancel) divergences

Practical simulation of LO, NLO and NNLO processes

Clearly an interplay between multiplicity of final states and order.
As an example, consider $pp \to Z + N$ jets with $N = 0, 1, 2$.

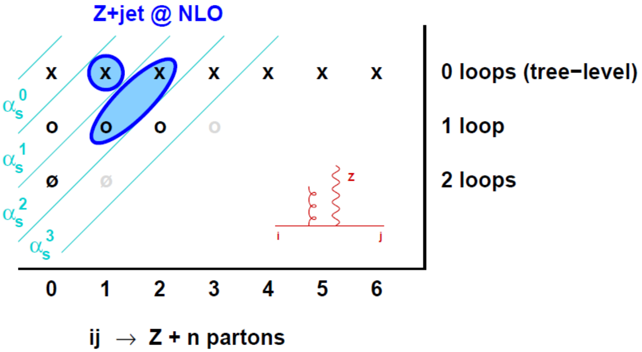

The bottleneck in getting N^{p}LO predictions is usually either the calculation of the p-loop diagram, or figuring out how to combine (cancel) divergences

Practical simulation of LO, NLO and NNLO processes

Clearly an interplay between multiplicity of final states and order.
As an example, consider $pp \to Z + N$ jets with $N = 0, 1, 2$.

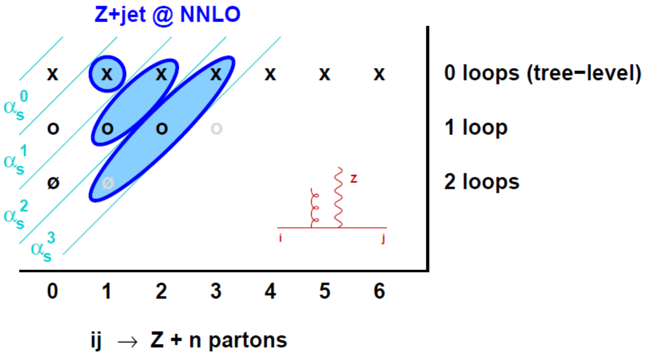

The bottleneck in getting N^{p}LO predictions is usually either the calculation of the p-loop diagram, or figuring out how to combine (cancel) divergences

Practical simulation of LO, NLO and NNLO processes

Clearly an interplay between multiplicity of final states and order.
As an example, consider $pp \to Z + N$ jets with $N = 0, 1, 2$.

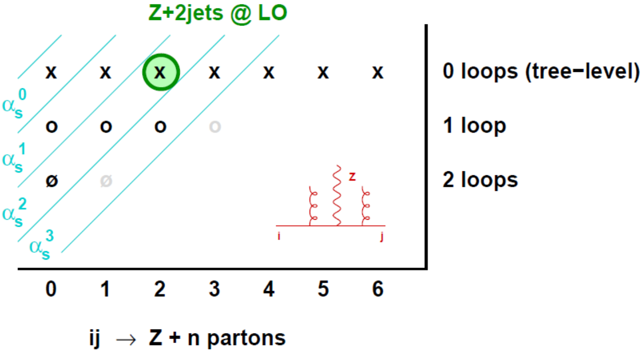

The bottleneck in getting N^{p}LO predictions is usually either the calculation of the p-loop diagram, or figuring out how to combine (cancel) divergences

Practical simulation of LO, NLO and NNLO processes

Clearly an interplay between multiplicity of final states and order.
As an example, consider $pp \to Z + N$ jets with $N = 0, 1, 2$.

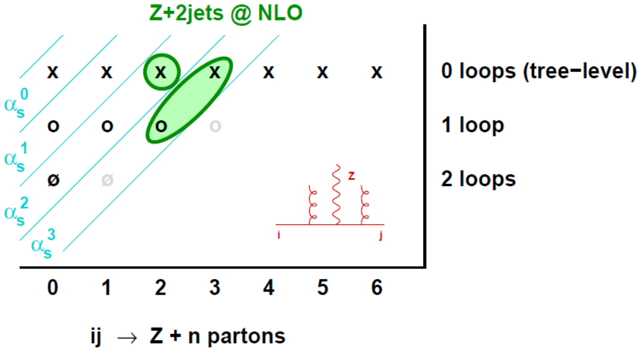

Cartoon from G. Salam lectures at Maria Laach

The bottleneck in getting N^{p}LO predictions is usually either the calculation of the p-loop diagram, or figuring out how to combine (cancel) divergences between 2 loops, 1 loop & tree level

Parton Shower and Hadronization

Also parton shower is simulated with MonteCarlo. Two main programs:
PYTHIA → Momentum ordering
HERWIG → Angular ordering
(also SHERPA and ARIADNE)
can be used also as hard scattering event generators.

Good description of "soft" processes

Hadronization. Clearly in the NP realm of QCD (happens at scale $Q_0 \sim \Lambda_{QCD}$)

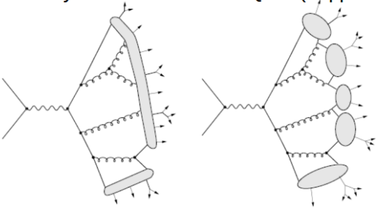

String (Lund) model (PYTHIA):
Color string across quarks and gluons

Cluster model (HERWIG and SHERPA):
Each gluon breaks in qq pair. Grouping quarks and antiquark in colourless clusters

Factorization (Theorem)

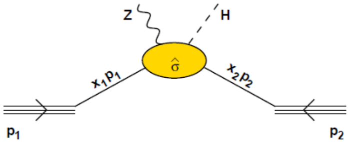

Cross section for $\sigma(pp \to ZH)$

Naive version:

$$\sigma = \int dx_1 f_{q/p}(x_1) \int dx_2 f_{\bar{q}/\bar{p}}(x_2) \hat{\sigma}(x_1 p_1, x_2 p_2)$$

Factorization:

- hard part $\hat{\sigma}(x_1 p_1, x_2 p_2)$
- non perturbative part from parton distribution functions (PDF)

At present we can't calculate PDF from first principles $\Rightarrow$ input from experimental fit (mainly Deep Inelastic Scattering experiments and neutrino scattering)

Deep Inelastic Scattering

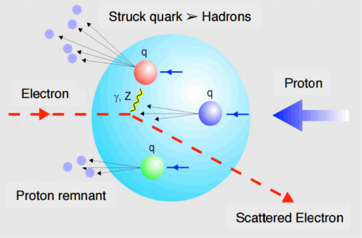

Since Rutherford's experiment, scattering is one of the most important tool to understand matter constituents.

DIS kinematics:

$$
\begin{aligned}
s &= (e+p)^2 \\
q &= e - e' \\
Q^2 &= -q^2 \\
y &= \frac{q \cdot p}{e \cdot p} \\
W^2 &= (q+p)^2 \\
x &= \frac{Q^2}{2p \cdot q}
\end{aligned}
$$

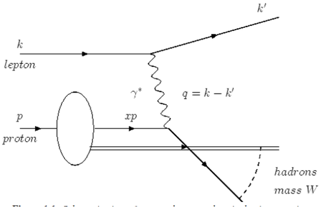

Use proton rest frame:

$$p = (M, \vec{0}) \; \nu = \frac{p \cdot q}{M} = E - E'$$

Measuring differential cross section:

$$\left(\frac{d^2\sigma}{dE' d\Omega}\right) = \left(\frac{d\sigma}{d\Omega}\right)_{Mott} \left\{ W_2(Q^2, x) + 2W_1(Q^2, x)\tan^2\left(\frac{\theta}{2}\right) \right\}$$

that can be rewritten as:

$$\frac{d\sigma}{dxdy} = \frac{4\pi\alpha^2 s}{Q^4}\left[xy^2 F_1 + (1-y)F_2\right]$$

with $F_1 = MW_1$ and $F_2 = \nu M_2$

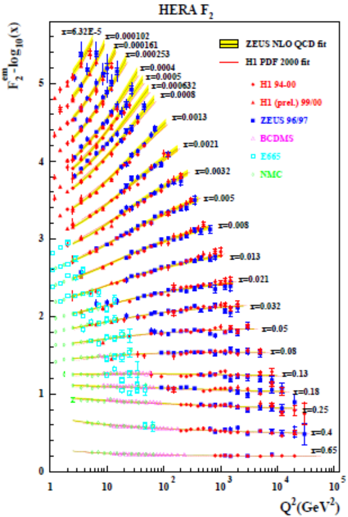

At large x F_2 is almost independent from q^2 $\Rightarrow$ Björken scaling.
Can also use W as probe in νp DIS

Parton Distribution Functions

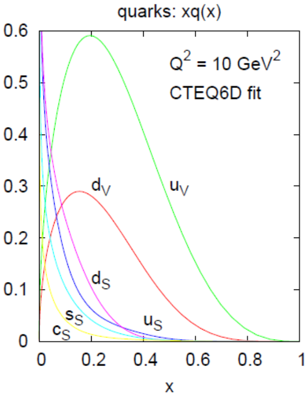

What is missing?

Check momentum sum-rule at (HERA collider *ep*):

$$\sum_i \int xq_i(x)dx = 1$$

u_v	0.267
d_v	0.111
u_s	0.066
d_s	0.053
s_s	0.033
c_c	0.016
Total	0.546

Parton Distribution Functions

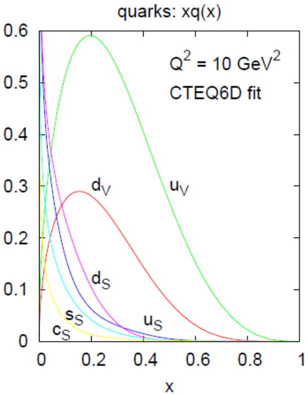

What is missing?
THE GLUON

Check momentum sum-rule at (HERA collider *ep*):

$$\sum_i \int x q_i(x) dx = 1$$

u_v	0.267
d_v	0.111
u_s	0.066
d_s	0.053
s_s	0.033
c_c	0.016
Total	0.546

Initial State Splitting

Evaluate cross section after hard process splitting occurs:

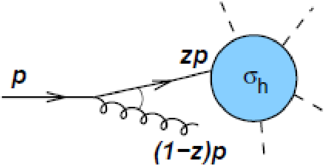

$$\sigma_{g+h}(p) \simeq \sigma_h(p) \frac{\alpha_s C_F}{\pi} \frac{dz}{1-z} \frac{dk_t^2}{k_t^2}$$

where $E = (1-z)p$

and $k_t = E \sin\theta \simeq E\theta$

We have to consider also virtual graphs:

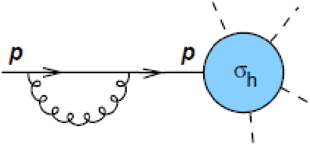

$$\sigma_{V+h}(p) \simeq -\sigma_h(p) \frac{\alpha_s C_F}{\pi} \frac{dz}{1-z} \frac{dk_t^2}{k_t^2}$$

Total contribution is:

$$\sigma_{g+h}(p) + \sigma_{V+h}(p) \simeq \frac{\alpha_s C_F}{\pi} \underbrace{\int_0^{Q^2} \frac{dk_t^2}{k_t^2}}_{divergent} \int_0^1 \underbrace{\frac{dz}{1-z}[\sigma_h(zp) - \sigma_h(p)]}_{finite}$$

BUT we can't go down to $k_t = 0$!

Collinear cut off

Limiting integral to μ_F^2 factorization scale (reminiscent to UV divergences treatment):

$$\sigma_0 = \int dx \sigma_h(xp) q(x, \mu^2)$$

$$\sigma_1 \simeq \frac{\alpha_s C_F}{\pi} \underbrace{\int_{\mu_F^2}^{Q^2} \frac{dk_t^2}{k_t^2}}_{finite!} \int_0^1 \underbrace{\frac{dxdz}{1-z}[\sigma_h(zp) - \sigma_h(p)] q(x, \mu_2)}_{finite}$$

DGLAP Evolution equations

DGLAP stands for: Dokshitzer, Gribov, Lipatov, Altarelli, Parisi

- G. Altarelli and G. Parisi. Nucl.Phys. B126:298 (1977)
- Y.L. Dokshitzer. Sov.Phys. JETP 46:641 (1977)
- V.N. Gribov, L.N. Lipatov. Sov.J.Nucl.Phys. 15:438 (1972)

Fix the outgoing quark momentum xp and take derivative wrt $\log \mu^2$. After some algebra:

$$\frac{dq(x,\mu^2)}{d\ln\mu^2} = \frac{1}{\delta}\left(\quad + \quad \right)$$

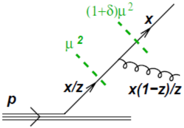

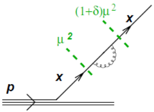

$$= \frac{\alpha_s}{2\pi}\int_x^1 dz P_{qq}\frac{q(x/z,\mu_F^2)}{z} - \frac{\alpha_s}{2\pi}\int_0^1 dz P_{qq}(z) q(x,\mu_F^2)$$

where $P_{qq}(z)$ is the quark splitting to a quark and a gluon. At first order:

$$P_{qq}(z) = C_F\frac{1+z^2}{1-z}$$

Full DGLAP

Full DGLAP evolution equation are obtained taking into account also gluon pdf.

$$\frac{d}{d\ln\mu^2} = \frac{\alpha_s(\mu_F^2)}{2\pi}\begin{pmatrix} P_{q\leftarrow q} & P_{q\leftarrow g} \\ P_{g\leftarrow q} & P_{g\leftarrow g}\end{pmatrix} \otimes \begin{pmatrix} q \\ g \end{pmatrix}$$

The splitting functions are (only at LO order!):

$$\begin{aligned}
P_{qq}(z) &= C_F\frac{1+z^2}{1-z} \\
P_{gq}(z) &= C_F\left[\frac{1+(1-z)^2}{z}\right] \\
P_{qg}(z) &= T_R[z^2+(1-z)^2] \\
P_{gg}(z) &= 2C_A\left[\frac{z}{(1-z)_+}+\frac{1-z}{z}+z(1-z)\right] \\
C_F &= \frac{4}{3}\,,\, C_A = 3\,,\, T_R = \frac{1}{2}
\end{aligned}$$

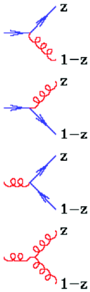

Coefficients are now known up to NNLO (crucial to have NNLO pdfs)

Splitting function at NLO

Splitting functions have been calculated at NLO:

$$\gamma_{\rm ns}^{(1)+}(N) = 4C_AC_F\left(2\mathbf{N}_+S_3 - \frac{17}{24} - 2S_{-3} - \frac{28}{3}S_1 + (\mathbf{N}_- + \mathbf{N}_+)\left[\frac{151}{18}S_1 + 2S_{1,-2} - \frac{11}{6}S_2\right]\right) + 4C_Fn_f\left(\frac{1}{12} + \frac{4}{3}S_1 - (\mathbf{N}_- + \mathbf{N}_+)\left[\frac{11}{9}S_1 - \frac{1}{3}S_2\right]\right) + 4{C_F}^2\left(4S_{-3} + 2S_1 + 2S_2 - \frac{3}{8} + \mathbf{N}_-\left[S_2 + 2S_3\right] - (\mathbf{N}_- + \mathbf{N}_+)\left[S_1 + 4S_{1,-2} + 2S_{1,2} + 2S_{2,1} + S_3\right]\right), \quad (3.5)$$

$$\gamma_{\rm ns}^{(1)-}(N) = \gamma_{\rm ns}^{(1)+}(N) + 16C_F\left(C_F - \frac{C_A}{2}\right)\left((\mathbf{N}_- - \mathbf{N}_+)\left[S_2 - S_3\right] - 2(\mathbf{N}_- + \mathbf{N}_+ - 2)S_1\right). \quad (3.6)$$

Splitting function at NNLO

and at NNLO too!

(and you have pages and pages of that!)

$$\begin{aligned}
\gamma_{\rm ns}^{(2)+}(N) \;=\; & 16 C_A C_F n_f \Big(\frac{3}{2}\zeta_3 - \frac{5}{4} + \frac{10}{9}S_{-3} - \frac{10}{9}S_3 + \frac{4}{3}S_{1,-2} - \frac{2}{3}S_{-4} + 2S_{1,1} - \frac{25}{9}S_2 \\
& + \frac{257}{27}S_1 - \frac{2}{3}S_{-3,1} - \mathbf{N}_+ \Big[S_{2,1} - \frac{2}{3}S_{3,1} - \frac{2}{3}S_4 \Big] - (\mathbf{N}_+ - 1)\Big[\frac{23}{18}S_3 - S_2\Big] - (\mathbf{N}_- + \mathbf{N}_+)\Big[S_{1,1} \\
& + \frac{1237}{216}S_1 + \frac{11}{18}S_3 - \frac{317}{108}S_2 + \frac{16}{9}S_{1,-2} - \frac{2}{3}S_{1,-2,1} - \frac{1}{3}S_{1,-3} - \frac{1}{2}S_{1,3} - \frac{1}{2}S_{2,1} - \frac{1}{3}S_{2,-2} + S_1\zeta_3 \\
& + \frac{1}{2}S_{3,1}\Big]\Big) + 16 C_F C_A^2 \Big(\frac{1657}{576} - \frac{15}{4}\zeta_3 + 2S_{-5} + \frac{31}{6}S_{-4} - 4S_{-4,1} - \frac{67}{9}S_{-3} + 2S_{-3,-2} \\
& + \frac{11}{3}S_{-3,1} + \frac{3}{2}S_{-2} - 6S_{-2}\zeta_3 - 2S_{-2,-3} + 3S_{-2,-2} - 4S_{-2,-2,1} + 8S_{-2,1,-2} - \frac{1883}{54}S_1 \\
& - 10S_{1,-3} - \frac{16}{3}S_{1,-2} + 12S_{1,-2,1} + 4S_{1,3} - 4S_{2,-2} - \frac{5}{2}S_4 + \frac{1}{2}S_5 + \frac{176}{9}S_2 + \frac{13}{3}S_3 \\
& + (\mathbf{N}_- + \mathbf{N}_+ - 2)\Big[3S_1\zeta_3 + 11S_{1,1} - 4S_{1,1,-2}\Big] + (\mathbf{N}_- + \mathbf{N}_+)\Big[\frac{9737}{432}S_1 - 3S_{1,-4} + \frac{19}{6}S_{1,-3} \\
& + 8S_{1,-3,1} + \frac{91}{9}S_{1,-2} - 6S_{1,-2,-2} - \frac{29}{3}S_{1,-2,1} + 8S_{1,1,-3} - 16S_{1,1,-2,1} - 4S_{1,1,3} - \frac{19}{4}S_{1,3} \\
& + 4S_{1,3,1} + 3S_{1,4} + 8S_{2,-2,1} + 2S_{2,3} - S_{3,-2} + \frac{11}{12}S_{3,1} - S_{4,1} - 4S_{2,-3} + \frac{1}{6}S_{2,-2} - \frac{1967}{216}S_2
\end{aligned}$$

PDFs **do vary** with Q^2 $\Rightarrow$ Scaling violation occurs increasing Q^2

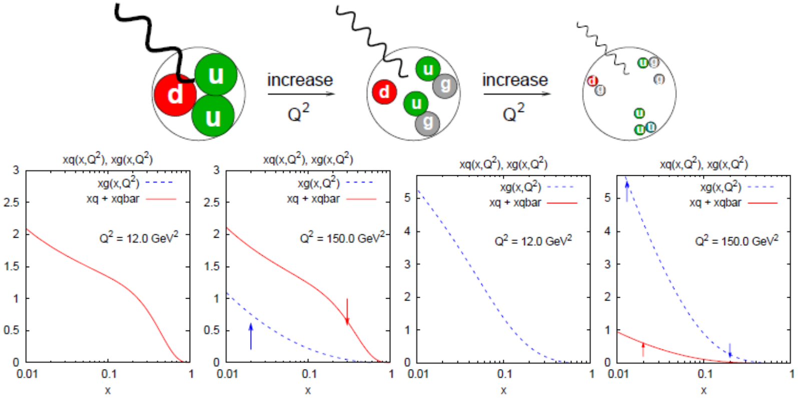

Parton Distribution Functions

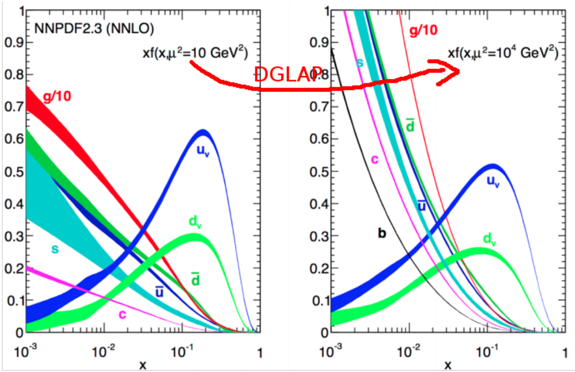

Many PDF sets available today (updates frequently):
MRST, CTEQ, NNPDF, HERAPDF,...
Available for LO, NLO and NNLO

Remarks:

- Valence quark distribution peak at larger x $\Rightarrow$ Heavy states preferentially produced by qq scattering rather than qq
- gluon distribution dominates at small-x PDF for valence quarks (harder) and sea quarks (softer).
- gluon (and sea quark) contribution increases at large Q^2 (DGLAP evolution)

From Hera to LHC

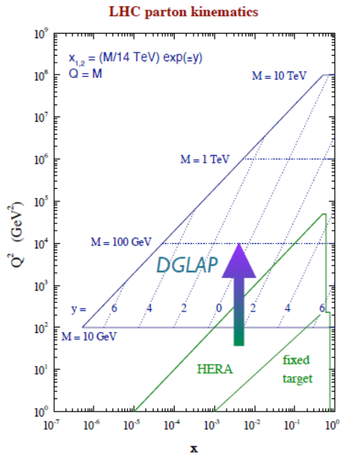

At HERA:

- *ep* collisions with $\sqrt{s_{ep}} \simeq 300\,GeV$ ($E(e) = 27.5$ GeV $E(p) = 920$ GeV
- Q^2 and x from kinematics (several methods)

At LHC:

- *pp* collider with $\sqrt{s} = 13$ TeV.
- Q^2 is the mass of the produced particle (*e.g.* for $t\bar{t}$ it is 350 GeV)
- Colliding x_1 and x_2 can be extracted in a $pp \to \Xi_M$ process with:

$$
\begin{aligned}
x_1 &= \frac{M_\Xi}{\sqrt{s}} e^{y_\Xi} \\
x_2 &= \frac{M_\Xi}{\sqrt{s}} e^{-y_\Xi} \\
y &= \frac{1}{2} \ln \frac{E + p_z}{E - P_z} \text{ (reminder)}
\end{aligned}
$$

DGLAP crucial to get the PDFs for LHC collider.
Small-x important at LHC for production of states with $\lesssim 100$ GeV
$x \simeq 1$ crucial for TeV state production (PBSM)

Factorization Theorem - Improved Version

Taking into account scaling violations:

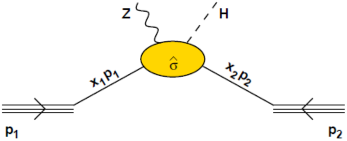

Cross section for $\sigma(pp \to ZH)$

Improved version:

$$\sigma = \int dx_1 f_{q/p}(x_1, \mu^2) \int dx_2 f_{\bar{q}/\bar{p}}(x_2, \mu^2) \hat{\sigma}(x_1 p_1, x_2 p_2, \frac{Q^2}{\mu^2})$$

Parton showers

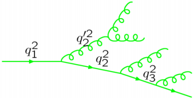

We need to calculate/model the momentum spectrum of gluons radiated from quarks. This is quite similar to DGLAP evolution equations since it involved the probability for a quark to radiate.

In the soft and collinear limit one can show that:

$$P(\text{no emission above } k_t) \simeq 1 - \frac{2\alpha_s C_F}{\pi} \int^Q \frac{dE}{E} \int^{\pi/2} \frac{d\theta}{\theta} \Theta(E\theta - k_T)$$

which gives at all order:

$$P(\text{no emission above } k_t) \equiv \Delta(k_T, Q) \simeq \exp\left[-\frac{2\alpha_s C_F}{\pi} \int^Q \frac{dE}{E} \int^{\pi/2} \frac{d\theta}{\theta} \Theta(E\theta - k_T) \right]$$

$\Delta(k_T, Q)$ is called Sudakov factor and it is used to calculate the distribution in K_T of gluons radiating off.

Interfacing LO (NLO) and Parton Shower

TOOLS FOR THEORETICAL PREDICTIONS

ME
Fixed order calculation
Limited number of final particles
Valid when partons are well separated and for multijet predictions

PS
No limit on final state multiplicity
Valid in soft or collinear regions
Needed for hadronization

Combine them!

Double Counting

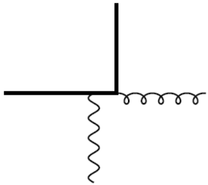

Z+parton

Double Counting

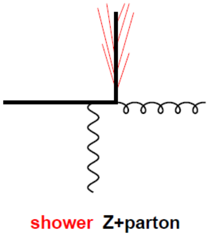

Double Counting

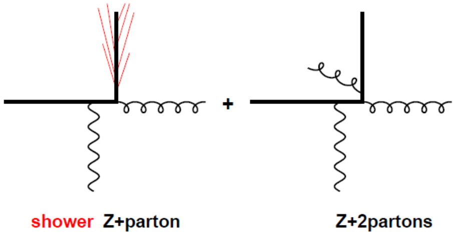

Double Counting

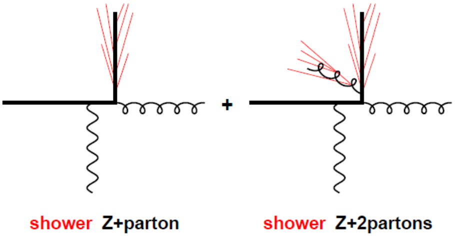

Double Counting

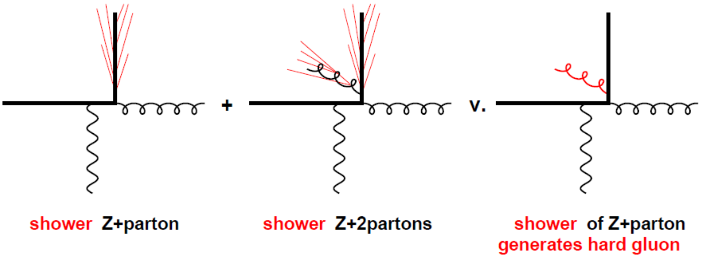

Double Counting

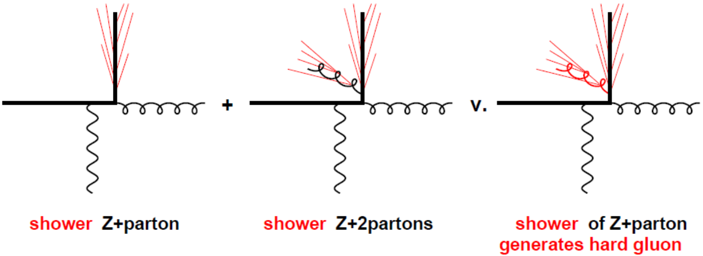

Clearly double counting in $Z + qq_{LO}$ and $Z + qq_{PS,hard}$.

Double Counting

Two recipes available to avoid *double counting*: MLM (M.Mangano)[hep-ph/0602031] and CKKW (Catani, Krauss, Kuhn, Webber) [hep-ph/0109231] and [hep-ph/0205283]
Main idea of MLM: hard jet ($P_T > P_{T,min}$) originates from hard scattering.

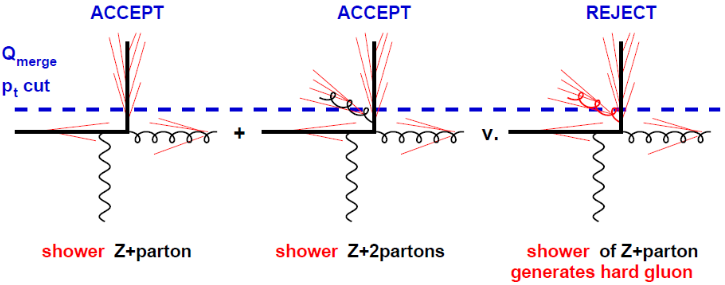

- Hard jets above scale Q_{merge} have distributions given by tree-level ME
- Rejection procedure eliminates "double-counted" jets from parton shower

Rutherford Experiment

Scattering is one of the most powerful tools of investigations of matter:
Probe: electron (point like)
Atom, nucleus, nucleon, quark & gluons is the object to be probed

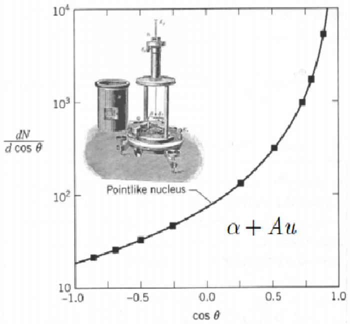

$$\frac{d\sigma}{d\Omega} = (zZ\alpha)^2 \left(\frac{\hbar c}{4E_{\rm kin}}\right)^2 \frac{1}{\sin^4(\theta/2)}$$

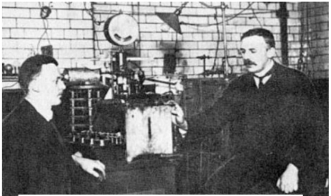

Rutherford Nobel Prize (chemistry)

Rutherford scattering: electrons on Au atoms.
Electron scattered by point like positive particles with potential V(r) = -1/r the nucleus

This is just classical mechanics (not even relativistic)

Mott Cross section

If electron mass can be neglected → relativistic formula → Mott formula

$$\left(\frac{d\sigma}{d\Omega}\right)_{\text{Mott}} = \frac{\alpha^2}{4E^2\sin^4\theta/2}\cos^2\frac{\theta}{2}$$

Rutherford formula with $E_K = E \quad (E \gg m_e)$

Overlap between initial/final state electron wave-functions. Just QM of spin ½

What happens if instead to point like charges we have a continous distribution of charges?

Potential is:

$$V(\vec{r}) = \int \frac{Q\rho(\vec{r}\,')}{4\pi|\vec{r}-\vec{r}\,'|}d^3\vec{r}\,' \quad \text{with} \quad \int \rho(\vec{r})d^3\vec{r} = 1$$

$$M_{fi} = \langle\psi_f|V(\vec{r})|\psi_i\rangle = \int e^{-i\vec{p}_3.\vec{r}}V(\vec{r})e^{i\vec{p}_1.\vec{r}}d^3\vec{r}$$

$= M_{fi} \times F(\vec{q}^2)$

with

$$F(\vec{q}^2) = \int \rho(\vec{r})e^{i\vec{q}.\vec{r}}d^3\vec{r}$$

Form Factors

For elastic scattering from a distributed charge the Mott cross section is multiplied by a form factor

$$\left(\frac{d\sigma}{d\Omega}\right)_{\text{Mott}} \rightarrow \frac{\alpha^2}{4E^2 \sin^4 \theta/2} \cos^2 \frac{\theta}{2} |F(\vec{q}^2)|^2$$

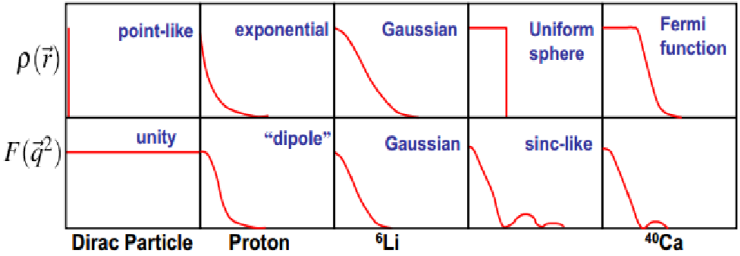

Increasing the Energy

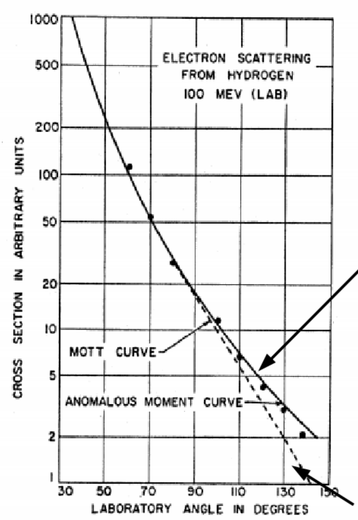

Hofstadter elastic scattering on Hydrogen Nuclei (E=100 MeV)

Mott and "anomalous" magnetic moment (1+k) with k=1.79

Mott: point like charge, no magnetic moment

Hofstadter elastic scattering on Hydrogen Nuclei (E=188 MeV)

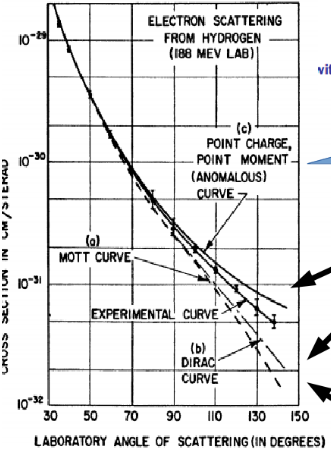

$$\frac{d\sigma}{d\Omega} = \frac{\alpha^2}{4E_1^2 \sin^4\theta/2} \frac{E_3}{E_1} \left(\frac{G_E^2 + \tau G_M^2}{(1+\tau)} \cos^2\frac{\theta}{2} + 2\tau G_M^2 \sin^2\frac{\theta}{2} \right)$$

vith the Lorentz Invariant quantity: $\tau = -\frac{q^2}{4M^2} > 0$

$$G_E(q^2) \approx G_E(\vec{q}^2) = \int e^{i\vec{q}.\vec{r}} \rho(\vec{r}) d^3\vec{r}$$

$$G_M(q^2) \approx G_M(\vec{q}^2) = \int e^{i\vec{q}.\vec{r}} \mu(\vec{r}) d^3\vec{r}$$

Modification for extended charge

Mott: point like charge, magnetic moment =1.79

Mott: point like charge, magnetic moment =1

$$\frac{d\sigma}{d\Omega} = \frac{\alpha^2}{4E_1^2 \sin^4\theta/2} \frac{E_3}{E_1} \left(\cos^2\theta/2 - \frac{q^2}{2M^2} \sin^2\theta/2 \right)$$

Mott: point like charge, no magnetic moment

Anomalous Magnetic moment

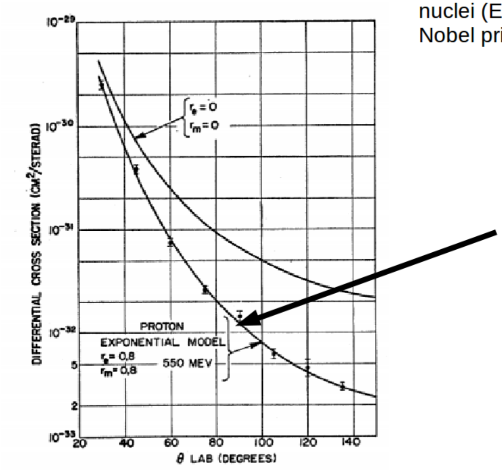

Hofstadter elastic scattering on H nuclei (E=550 MeV)
Nobel prize 1961

Measures proton size
Nobel Prize 1961

Higher probe energies

Now increase the energy of electron beam
5 GeV< Ebeam< 20 GeV (SLAC)

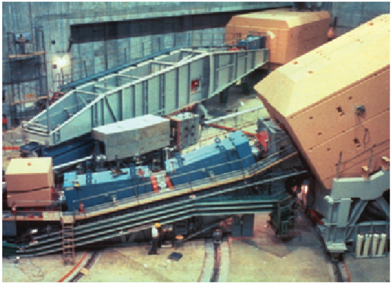

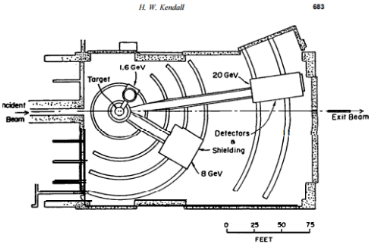

Deep Inelastic Scattering

DIS kinematics:

$$
\begin{aligned}
s &= (e+p)^2 \\
q &= e - e' \\
Q^2 &= -q^2 = 4EE'\sin^2(\theta/2) \\
\nu &= E - E' \\
y &= \frac{q\cdot p}{e\cdot p} = \frac{\nu}{E} \\
W^2 &= (q+p)^2 \\
&= M^2 - Q^2 + 2M\nu \\
x &= \frac{Q^2}{2p\cdot q} = \frac{Q^2}{2M\nu}
\end{aligned}
$$

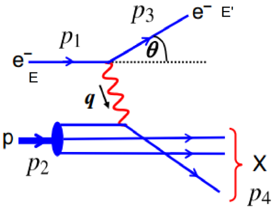

Use proton rest frame:

$$p = (M, \vec{0})\ \nu = \frac{p\cdot q}{M} = E - E'$$

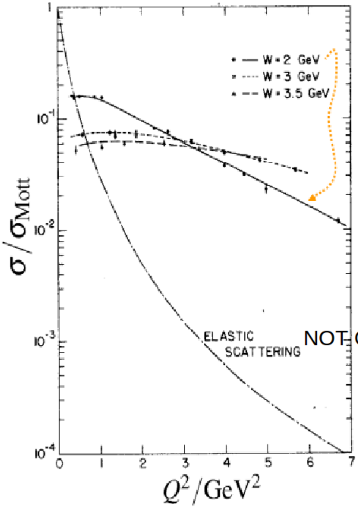

~Almost flat in Q^2 ! → Scattering of Point like objects in the proton

OBSERVED

NOT OBSERVED!

Scaling

Generalized Rosenbluth formula for elastic scattering can be rewritten in terms of reativistically invariant is:

$$\frac{d\sigma}{dQ^2} = \frac{4\pi\alpha^2}{Q^4}\left[\frac{G_E^2+\tau G_M^2}{(1+\tau)}\left(1-y-\frac{M^2y^2}{Q^2}\right)+\frac{1}{2}y^2G_M^2\right]$$

which can be written as:

$$\frac{d\sigma}{dQ^2} = \frac{4\pi\alpha^2}{Q^4}\left[f_2(Q^2)\left(1-y-\frac{M^2y^2}{Q^2}\right)+\frac{1}{2}y^2f_1(Q^2)\right]$$

In Deep inelastic scattering we hve two independent variables x and Q^2:

$$\frac{d^2\sigma}{dx dQ^2} = \frac{4\pi\alpha^2}{Q^4}\left[\left(1-y-\frac{M^2y^2}{Q^2}\right)\frac{F_2(x,Q^2)}{x}+y^2F_1(x,Q^2)\right]$$

$F2(x,Q^2)$ and $F1(x,Q^2)$ are not anymore form factors but are momentum distributions of constituents of the proton.
In the high energy limit $Q^2 >> M^2Y^2$

$$\frac{d^2\sigma}{dx dQ^2} = \frac{4\pi\alpha^2}{Q^4}\left[(1-y)\frac{F_2(x,Q^2)}{x}+y^2F_1(x,Q^2)\right]$$

Electromagnetic
Pure magnetic

Experimentally:

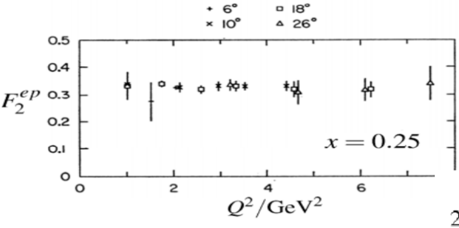

Independent from Q^2

Same for F1

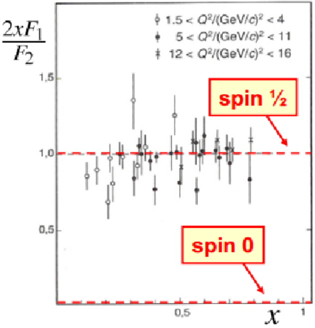

If spin ½ $F_2(x) = 2x\, F_1(x)$

Callan-Gross relation

Measuring differential cross section:

$$\left(\frac{d^2\sigma}{dE' d\Omega}\right) = \left(\frac{d\sigma}{d\Omega}\right)_{Mott}$$
$$\left\{W_2(Q^2,x) + 2W_1(Q^2,x)\tan^2\left(\frac{\theta}{2}\right)\right\}$$

that can be rewritten as:

$$\frac{d\sigma}{dxdy} =$$
$$= \frac{4\pi\alpha^2 s}{Q^4}\left[xy^2F_1 + (1-y)F_2\right]$$
with $F_1 = MW_1$ and $F_2 = \nu M_2$

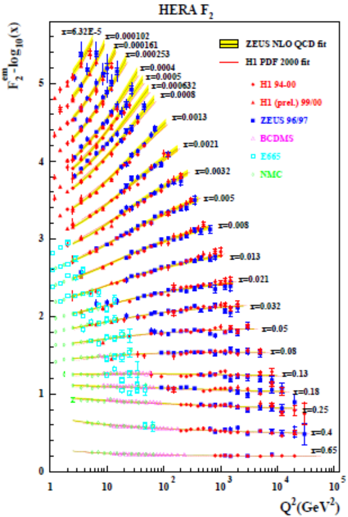

At large x F_2 is almost independent from q^2 $\Rightarrow$ Björken scaling.
Can also use W as probe in νp DIS

From Hera to LHC

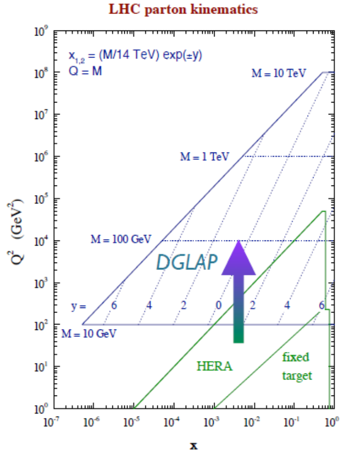

At HERA:

- *ep* collisions with $\sqrt{s_{ep}} \simeq 300\,GeV$ $(E(e) = 27.5\ \text{GeV}\ E(p) = 920\ \text{GeV}$
- Q^2 and x from kinematics (several methods)

At LHC:

- *pp* collider with $\sqrt{s} = 13\ \text{TeV}$.
- Q^2 is the mass of the produced particle (*e.g.* for $t\bar{t}$ it is 350 GeV)
- Colliding x_1 and x_2 can be extracted in a $pp \to \Xi_M$ process with:

$$x_1 = \frac{M_\Xi}{\sqrt{s}} e^{y_\Xi}$$

$$x_2 = \frac{M_\Xi}{\sqrt{s}} e^{-y_\Xi}$$

$$y = \frac{1}{2} \ln \frac{E + p_z}{E - P_z} \text{ (reminder)}$$

DGLAP crucial to get the PDFs for LHC collider.
Small-x important at LHC for production of states with $\lesssim 100\ \text{GeV}$
$x \simeq 1$ crucial for TeV state production (PBSM)

Table of Contents

In a detector

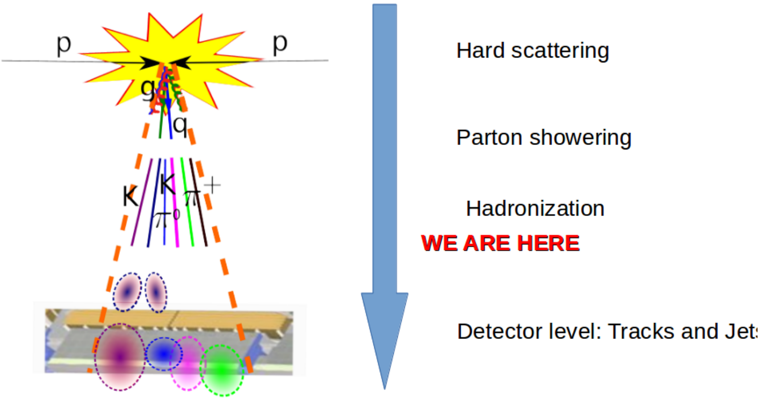

Hadronic Jets

Jet algorithm reconstruction → Clustering of:
Physics objects from detector:
calorimeter deposits, tracks or combination
MC Truth:
After parton showering (parton level)
After hadronization (particle level)

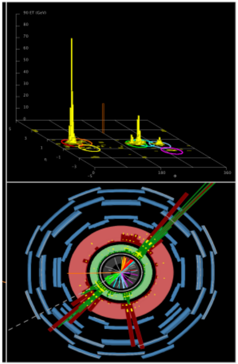

Clear 2-jet event

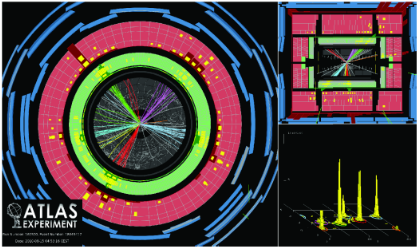

4, 5 or 6 jet event?

Clustering Algorithms

Jet clustering algorithms need to define:
Which particles/objects do we cluster together and which we don't
How we combine the momentum ? (4-momentum sum is most obvious)

Byproduct (necessary): A method to condense information (several thousands of particles → less than 10 jets)

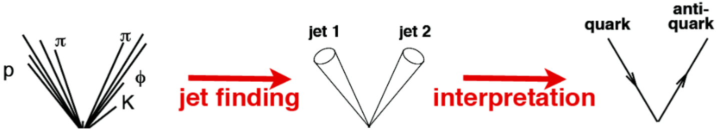

Jet reconstruction algorithms need to be:

- Reminiscent of the partons that produced them
- Well defined from a theoretical point of view (insensitive to soft and collinear radiation)
- Computationally no too CPU heavy

IRC Safety

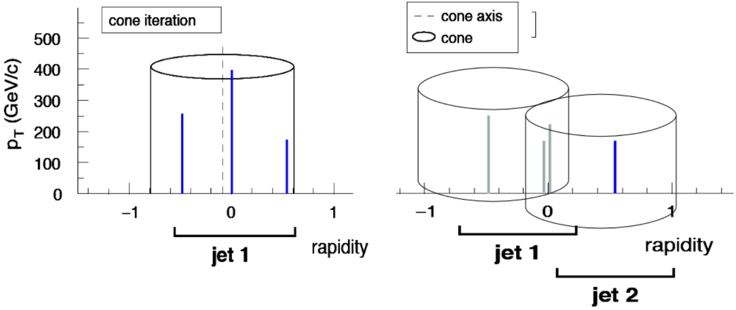

Simple iterative one jet is **NOT** infrared safe
Because "hardest" particle is not a IR safe quantity (in particular unsafe for colinear splitting)

Seedless cone (SiS) are IRC safe but let's focus on kT algorithms

K_T Jet Algorithms

Sequential algorithms are iterative procedures that try to reverse the pattern of QCD gluon radiation $\Rightarrow$ IRC safer.
Metrics definition for all i, j *physics objects* define distance d_{ij} and a *magnitude* d_{iB}: and a :

$$
\begin{aligned}
d_{ij} &= \min(p_{Ti}^{2p}, p_{Tj}^{2p})\frac{\Delta R_{ij}^2}{R^2}, \ \Delta R_{ij}^2 = (y_i - y_j)^2 + (\phi_i - \phi_j)^2 \\
d_{iB} &= p_{Ti}^{2p}
\end{aligned}
$$

1. Choose parameter R $(0.4 \leq R \leq 1.2)$
2. Evaluate d_{ij} and d_{iB} $\forall (i, j)$ pairs and i particles
3. Find the minimum between d_{ij} and d_{iB}
   - If it is $d_{ij} \Rightarrow$ combine together i and j and go back to 1
   - If it is $d_{iB} \Rightarrow$ i is a jet and remove from list
4. Stop when no particles remain

Depending on p exponent:

- $p = 1 \Rightarrow$ Classical k_T. Favors clustering of soft particles
- $p = 0 \Rightarrow$ Cambridge/Aachen (CA). Clustering energy independent.
- $p = -1 \Rightarrow$ *anti-K_T*. Favors clustering of hard particles

Different Jet Clustering at Work

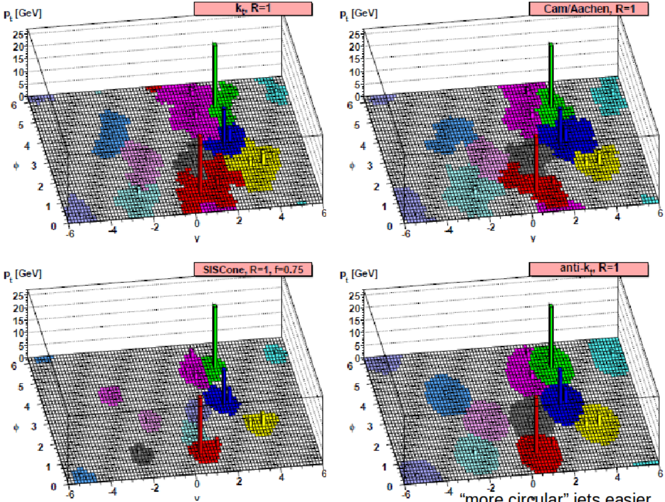

from G,P Salam arXiv:0906.1833

"more circular" jets easier to handle experimentally

Optimization

Optimization:
How to choose jet algorithm?
How to choose parameters (e.g. R)?

It depends from:
1) Detector (granularity, energy resolutions)
2) Experimental conditions (pileup, background)
3) Is it a precision measurement or a search? How much background do you expect
4) Kinematics of the event (is it a high mass state ~1TeV or ~100 GeV?)
5) Is it a gluon, a light quark or a heavy quark jet?

Anaytical optimization
from G,P Salam arXiv:0906.1833

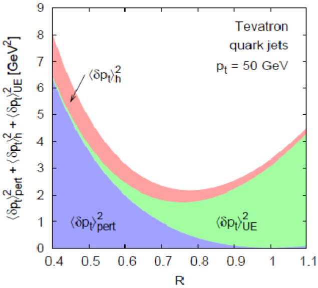

Larger R → means more acceptance, smaller corrections, better energy resolutions → Larger statistics

In presence of pileup or noise, large R → increased probability to collect energy flow NOT from interesting events

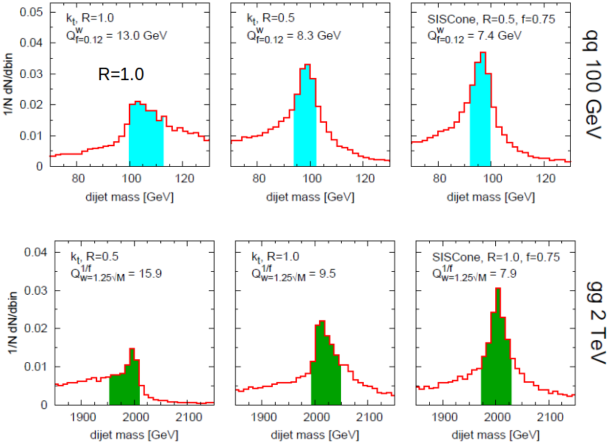

from Cacciari, Rojo and Salam arXiv:0810.1304

Different trend for gluon jets than quark jets

Jet Measurements at LHC

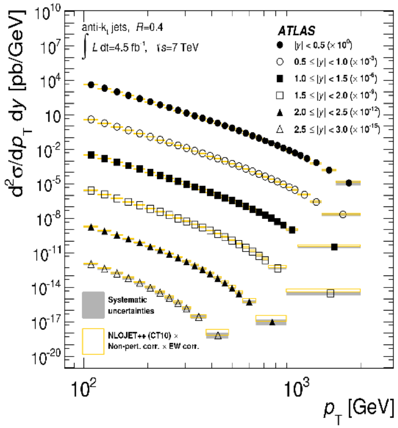

from JHEP02(2015)153

Inclusive jet production cross section
Measured by ATLAS at √s=7 TeV (Run1) (also at 8 TeV and 2.76 TeV)

Double differential cross section (in P_T and y)

Quite accurate test of:
- pQCD (NLO) up to ~1TeV (different PDF sets were checked)
- Understanding of experimental problematics
- Additional measurements: dijets, tri-jets etc... with or w/o Heavy Flavours → additional constraints on PDF

Boosted jets

Some kinematics $m_1, m_2 \simeq 0$:

$$
\begin{aligned}
m^2 &= 2E_1E_2(1-\cos\theta_{12}) \\
m^2 &= \frac{E^2}{2}(1-\cos\theta_{12}) \text{ if } E_1 = E_2 = \frac{E}{2} \\
4\frac{m^2}{E^2} &= \theta_{12}^2 \text{ for small } \theta_{12} \\
\theta_{12}^2 &= 2\frac{m}{E} = \frac{2}{\gamma}
\end{aligned}
$$

$\Rightarrow$ jet from a $N-$body decay need to be large and has some substructure that can be used to reduce contribution from *normal* jets.

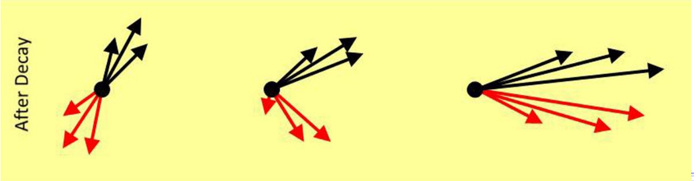

Boosted taggers

Very active research area at the moment → Impact on top, exotic and Higgs physics

Example: Trimming (ATLAS: $R_{sub} = 0.3$, $f_{cut} = 0.05$)

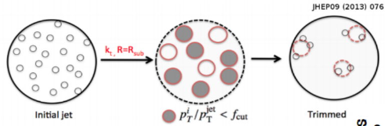

Motivations for the plethora of sub-jetness algorithms are based on QCD. Strategy is to remove soft QCD components and keep the hard ones

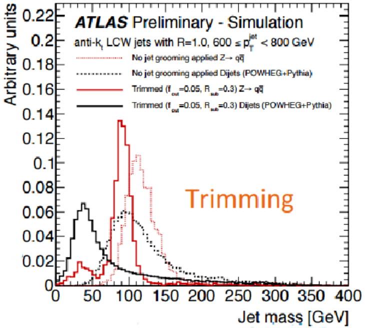

Boosted taggers

Specific taggers designed to:

- Remove QCD
- Keep and tag hadronic decays of W, boosted top quark and even Higgs

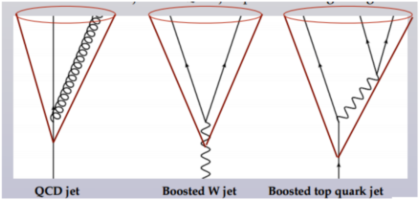

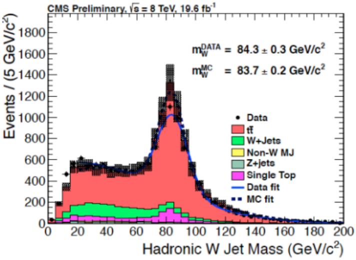

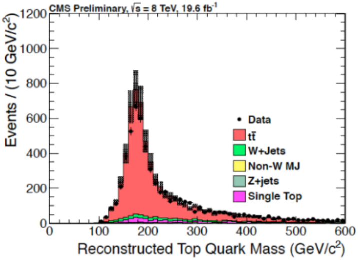

from CMS PAS JME-13-007

ATLAS Calorimetry

ATLAS Calorimeters
A complex system with fine granularity segmented in 3D

Electromagnetic calorimeter
- Barrel (LAr-Pb) |η|<1.4
- EndCap (LAr-Pb) 1.375<|η|<3.2

Hadronic calorimeter
- Barrel (Tile) |η|<1.7
- EndCap (LAr-Cu) 1.5<|η|<3.2

Forward: (LAr) 3.2<|η|<4.9

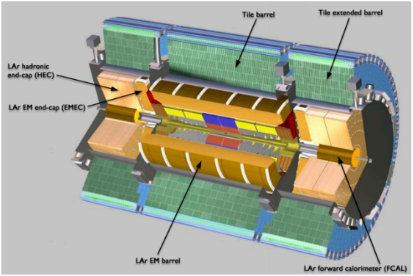

$$\frac{\sigma_E}{E} = \frac{a}{\sqrt{E}} \oplus \frac{b}{E} \oplus c$$

a: Sampling fluctuations, leakage fluctuations

b: inhomogeneities, shower leakage

c: electronic noise , sampling fraction variations

Typical values:

a: 0.5 ~ 1.0

b: 0.03~0.05

c: few %

more on Detector lectures

Jet Calibration

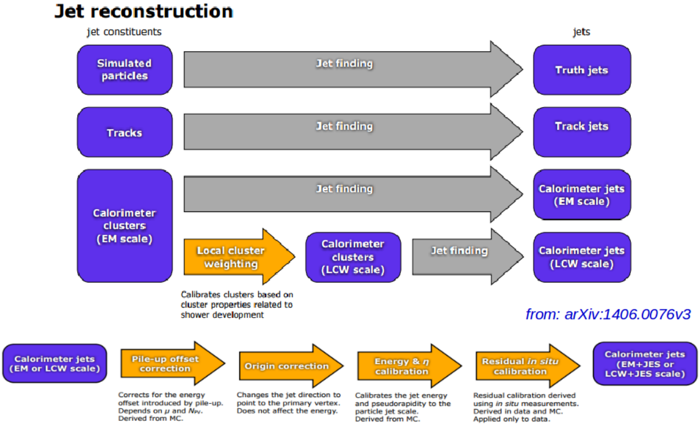

To be repeated for all supported jet algorithms and radius R !

Complex procedure that uses both MC simulations and *in-situ* data

TopoClusters: clusters of calorimeter towers 3D (η,ϕ,R)

Seed: $|E_{cell}|>4\ \sigma_{noise}$

Neighbours: $|E_{cell}|>2\ \sigma_{noise}$

Perimeter cells: $|E_{cell}|>0$

Noise: Electronic ⊕ PileUp

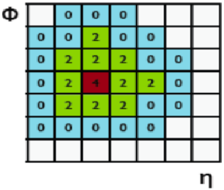

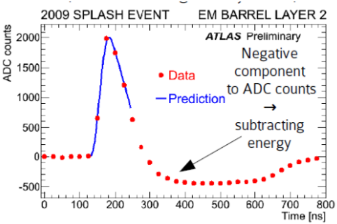

Pile Up Noise:
InTime: extra interactions within the same bunch crossing
Out of Time: additional energy deposits from previous bunch crossing

PileUp Corrections

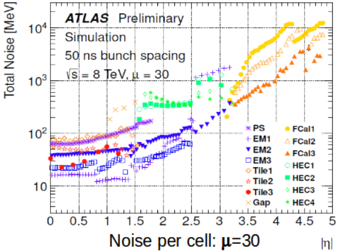

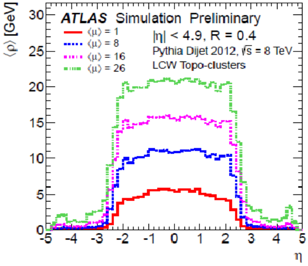

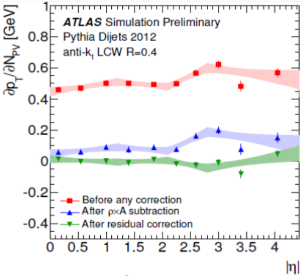

Energy is subtracted using jet area

$$\rho = \text{median}\left\{\frac{p_{T,i}^{jet}}{A_i^{jet}}\right\}$$

$$p_T^{corr} = p_T^{jet} - \rho \times A^{jet}$$

Jet Area subtraction:

- Circular area jets (anti-kT) are better
- Energy correction cannot get rid of whole jets

from ATLAS-CONF-2014-018 and paper in preparation (EPJC)

ATLAS Jet Vertex Tagger

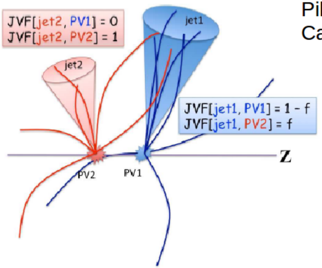

Pile up events can also add whole jets.
Cannot subtract them with area

Use tracking information to reject jets produced by pile up event

$$\mathrm{corrJVF} = \frac{\sum_k p_T^{\mathrm{trk}_k}(\mathrm{PV}_0)}{\sum_l p_T^{\mathrm{trk}_l}(\mathrm{PV}_0) + \frac{\sum_{n\geq 1}\sum_l p_T^{\mathrm{trk}_l}(\mathrm{PV}_n)}{(k\cdot n_{\mathrm{trk}}^{\mathrm{PU}})}}.$$

$$R_{p\mathrm{T}} = \frac{\sum_k p_T^{\mathrm{trk}_k}(\mathrm{PV}_0)}{p_T^{jet}}.$$

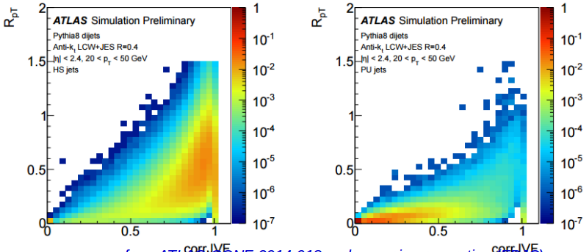

from ATLAS-CONF-2014-018 and paper in preparation (EPJC)

ATLAS Jet Vertex Tagger

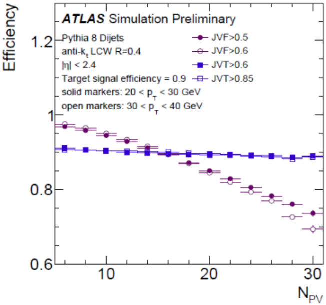

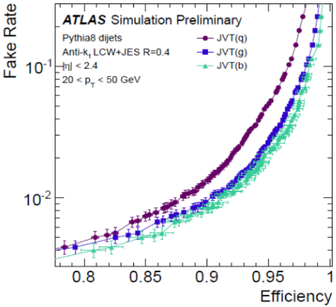

from ATLAS-CONF-2014-018 and paper in preparation (EPJC)

In-situ calibrations

In Situ calibration:

Correction factor $\langle P_T^{Jet}/P_T^{Ref}\rangle_{Data} / \langle P_T^{Jet}/P_T^{Ref}\rangle_{MC}$

Different methods to cover different kinematic regions

Dijet η-calibration: Equalize P_T^{Jet} in central and forward regions

γ/Z + jet dibalance calibration: γ measured with better accuracy, Z boson P_T^{Jet} measured from tracking

Multijet Balance: P_T jet system recoils against a high P_T jet used to calibrate jets in the TeV regime

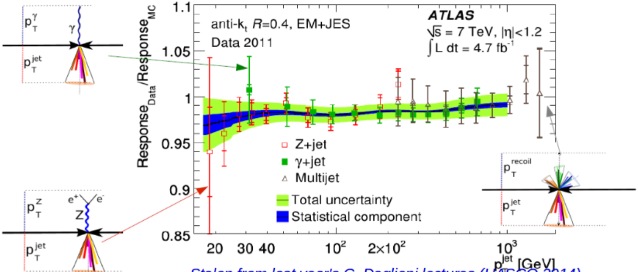

Stolen from last year's C. Doglioni lectures (HASCO 2014)

from: arXiv:1406.0076v3

Jet Energy Scale (JES) Uncertainties

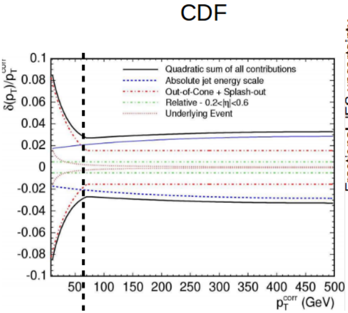

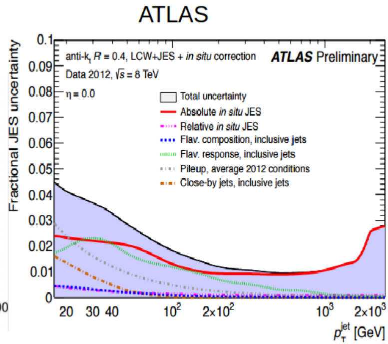

from: arXiv:1406.0076v3

IN ATLAS Total uncertainties never larger than 5%
In most energy range ~ 2%

Perturbative *vs* Non Perturbative QCD

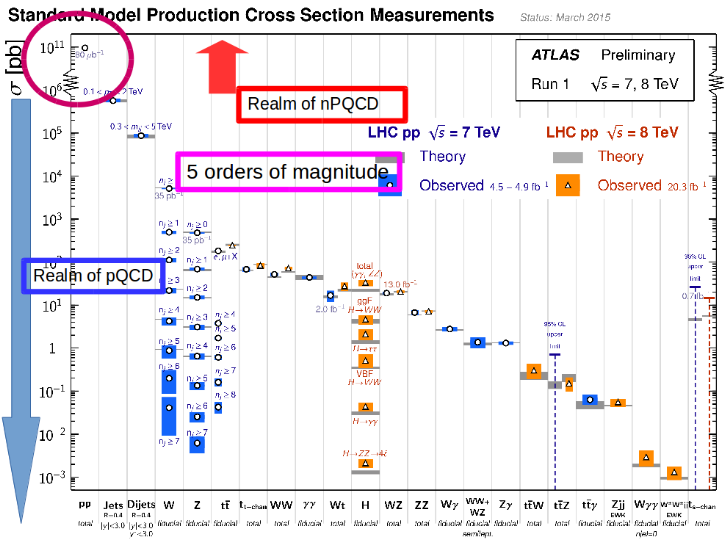

NP-QCD Measurements

Experimental QCD doesn't end with Perturbative QCD (and jets)!
There is much more than that!

- Non Perturbative QCD is:
- Proton-proton cross section measurement
- Minimum bias event characterization
- Underlying event characterization
- Diffractive physics

→ This covers more than 99.9999etc...% of the LHC production cross section!

proton-proton cross section

Inelastic **σ**(pp) cross section measruement. Two methods:

- Measure cross section in fiducial region

$$\sigma = \frac{N - Bkg}{\varepsilon \times Acc \times \int \mathcal{L}\, dt}$$

selection very loose:

just to select events from collisions

Small background (beam-halo etc....)

→ Extrapolate to full acceptance → Large uncertainties

- Use optical theorem

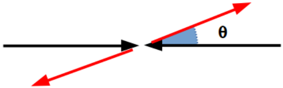

$$\sigma_{\text{tot}} = 4\pi \cdot Im\left(f_{\text{el}}(0)\right)$$

$$\sigma^2_{tot} = \frac{16\pi(\hbar c)^2}{1+\rho^2} \frac{d\sigma_{el}}{dt}\bigg|_{t=0}$$

Need to go to small t to extrapolate to t=0

$\rho = \mathfrak{Re}[fel(0)]/\mathfrak{Im}[fel(0)]$

→ from theory

Diffraction at hadron colliders

Theory:
Interactions where the beam particles (one or both) emerge intact or dissociated into low mass states.

OR

Interactions mediated by t-channel exchange of object (ladder of gluons) with the quantum numbers of the vacuum, i.e. color singlet exchange called "Pomeron"

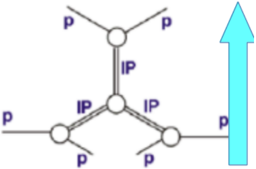

Experimentally:
- No energy/momentum flow in "forward regions" → Rapidity gaps
- Tag one or both protons in the final state ("very very close" to beam axis) → ALFA, AFP (ATLAS), TOTEM (CMS)

Kinematics is determined by:

- t → 4-momentum exchanged by protons
- Mass of diffractive system (M_X)

$$\sigma_{Total} = \sigma_{Elastic} + \sigma_{Inel}$$
$$= \sigma_{Elastic} + \sigma_{ND} + \sigma_{SD} + \sigma_{DD} + \sigma_{CD}$$

$$\xi = M_X^2 / s$$

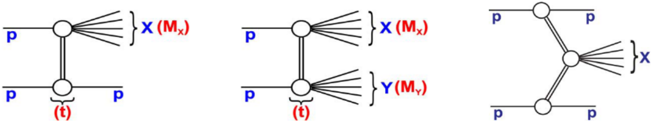

Single Diffractive (SD) ~ 14mb

Double Diffractive (DD) ~9 mb

Central Diffractive (CD) ~ 10% of SD

Diffraction Cartoon

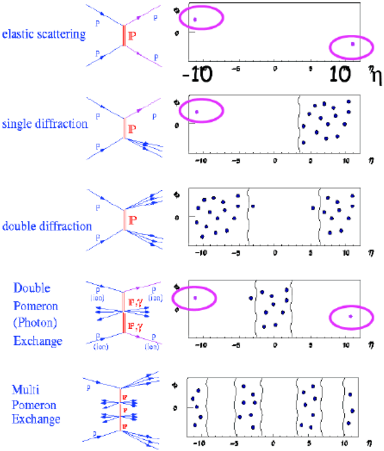

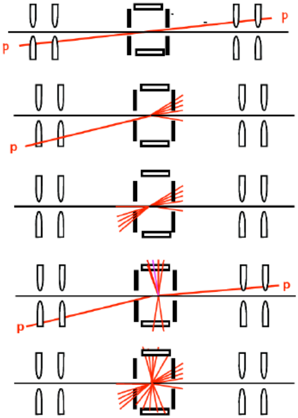

For Non Diffractive events $dN/d\eta \sim 6$ and $<\eta_j - \eta_k> \sim 0.15$

→ Large η gaps are exponentially suppressed except for Diffractive events

Measuring $\Delta\eta$ is a measurement of $M_{X(y)}$

$$\Delta\eta = \ln s/M_X^2 = -\ln\xi$$

Difficult measurement of $M_{X(Y)}$ → Produced particles escape undetected in the beam pipe

η acceptance is defined in the largest η range $-4.9<\eta<4.9$

→ However max η gap determined by MBTS position (→ trigger) (Max $\Delta\eta \sim 8$)

Using ID+EM+HEC+FCAL

$0<\Delta\eta^F<8$ → $\sim 10^{-6} < \xi < \sim 10^{-2}$ → ~ 7 GeV $< M_x <$ ~ 700 GeV

Experimentally (detector) η rings (variable width 0.2, 0.4 according to η region):

Active ring if:

- At least one track with P_T>200 MeV (also checked P_T threshold=400,600,800 MeV/c)
- At least one calorimeter cell above noise threshold (η-dependent threshold, no noise in Tile calorimeter) and E_T cut (same as track)

Asymmetric Events

Asymmetric events:
→ Measure R_{ss}: ratio of **single sided** MBTS events wrt total inelastic events

$$R_{ss} = \frac{N_{ss}}{N_{incl}}$$

From R_{ss} → Measure ratio

$$f_D = \frac{\sigma_{DD} + \sigma_{SD} + \sigma_{CD}}{\sigma_{Inel}}$$

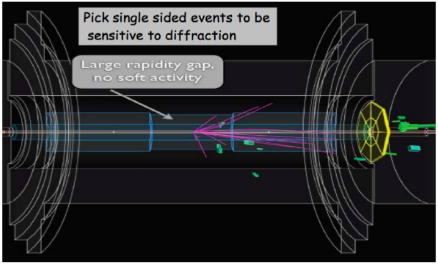

f_D is one of the key components of the total inelastic cross section measurement

$$\sigma_{incl} = \frac{N - N_{bg}}{\epsilon \times A_{inel} \times \int \mathcal{L} dt}$$

$\int \mathcal{L}\, dt = 20\ \mu b^{-1}$

Measured $R_{ss} = 10.02 \pm 0.03\ (stat)^{+0.1}_{-0.4}\ (syst)\ \%$

Several models

$R_{ss} \rightarrow$ Constraint f_D for each

$f_D = 26.9^{+2.5}_{-1.0}\ \%$

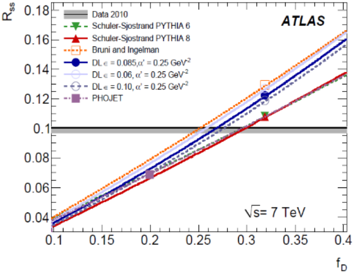

for Pythia 8 +DL with ξ dependence parametrized with pomeron intercept:

$\alpha(t) = \alpha(0) + \alpha' t$

With $\alpha' = 0.25\,\mathrm{GeV}^{-2}$

$\varepsilon = \alpha(0) - 1 = 0.085$

$$\frac{d\sigma_{SD}}{d\xi} \sim \frac{1}{\xi^{(1+\varepsilon)}} (1+\xi)$$

Measured cross section is for $\xi > 5 \times 10^{-6}$

$$\xi = \frac{M_X^2}{s} > 5 \times 10^{-6} M_X > 15.7\,\mathrm{GeV}$$

$$\sigma_{inel}(\xi > 5 \times 10^{-6}) = \sigma_{inel} \times (1 - f_{\xi < 5\times 10^{-6}})$$

$$\xi > m_p^2/s$$

Use DL MC to extrapolate to full range

$\sigma(\xi > 5\times10^{-6}) = 60.33 \pm 2.10$ mb ($M_x > 15.7$ GeV)

$\sigma(\xi > m^2_p/s) = 69.4 \pm 2.4 \pm 6.9(\mathrm{extr})$ mb

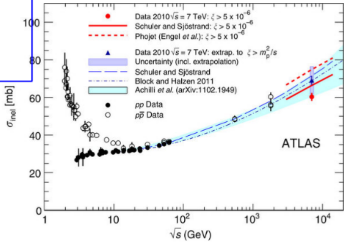

Nature Comm. ***2*** *(2011) 463*

$\sigma(pp)$ vs $\sqrt{s}$

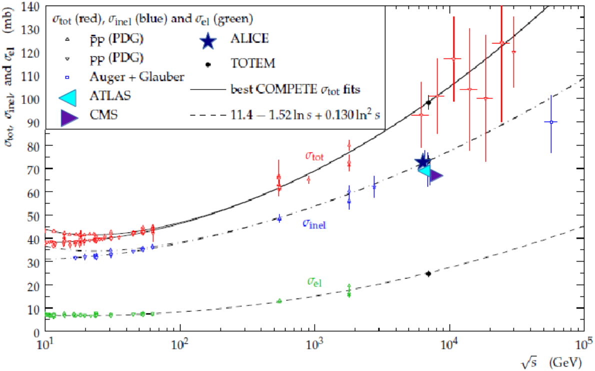

Measuring $\sigma(pp)$ with ALFA

To be able to go to small t → small angles:

- Go far (in z) (more than 200m from IP)
- Go close to the beam (→ need special beam conditions → high **β***)
- and NO PILE UP!
- (ALFA is hosted in Roman Pot)

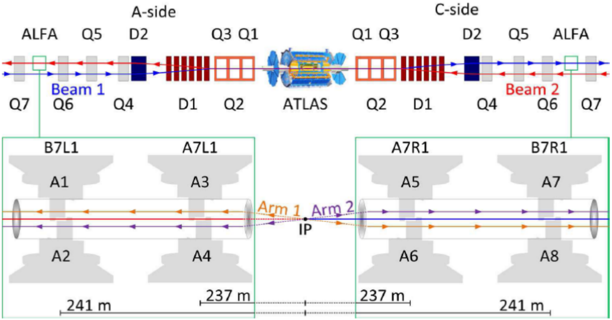

CMS has similar detector: TOTEM

Measuring $\sigma(pp)$ with ALFA

To be able to go to small t → small angles:

- Go far (in z) (more than 200m from IP)
- Go close to the beam (→ need special b… …ns → high β*)
- and NO PILE UP!
- (ALFA is hosted in Roman Pot)

Wait! Roman pots??

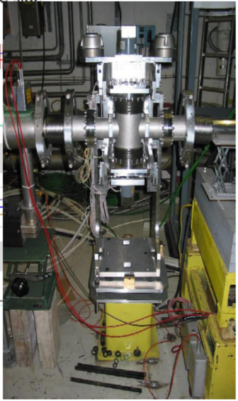

Experimental Issues

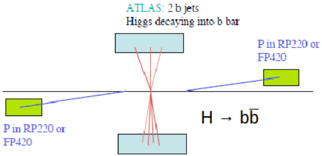

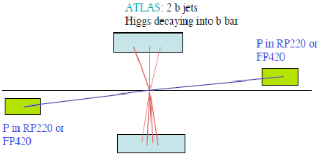

Diffractive H → bb̄

- PileUp
- Specific LHC fills with specific optics (large β*) → Low luminosity
- Move the devices close to beam (few mm) → Beams **ABSOLUTELY** stable
- When running with the whole detector → time latency issues:

Protons have to travel 240m + signals have to travel 240m back to ATLAS for TDAQ

→ Event fragments collected by the ATLAS subdetectors might be close to the L1 latency (2.5μs) → Need to run ATLAS TDAQ with extended latency (+20BC=+250ns) All but muon detectors can accommodate that

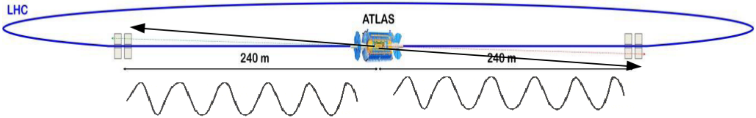

ALFA detector

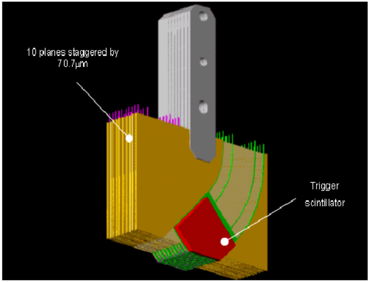

Schematic of ALFA detector
Tracking device made with cintillating fibers
Movable devices go close to the beam ! (10 σ of beam width → few mm)

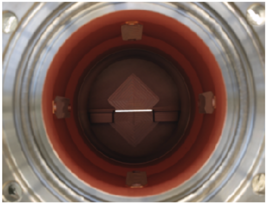

Tracking in ALFA

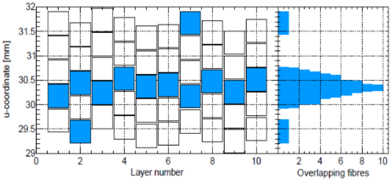

$\frac{d\sigma}{dt}$

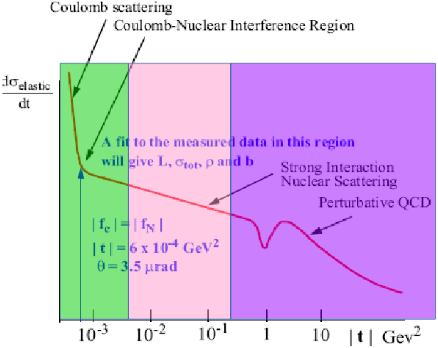

Extrapolation for t=0 → Min Reachable t:

~0.3~1 GeV^2 β*=0.5m,3m (Standard pp runs)

~10^{-2} GeV^2 β*=90m (2011/2012 special runs)

~10^{-4} GeV^2 β*=2900m (later)

details in accelerator lectures

$\frac{d\sigma}{dt}$

$$\frac{d\sigma}{dt} = \frac{4\pi\alpha^2(\hbar c)^2}{|t|^2} \cdot G^4(t) \quad \text{Coulomb}$$

$$\text{CNI} \quad - \quad \sigma_{\text{tot}} \cdot \frac{\alpha G^2(t)}{|t|} \left[\sin(\alpha\phi(t)) + \rho\cos(\alpha\phi(t))\right] \cdot \exp\frac{-B|t|}{2}$$

$$\text{Nuc.} \quad + \quad \sigma_{\text{tot}}^2 \frac{1+\rho^2}{16\pi(\hbar c)^2} \cdot \exp(-B|t|) \quad .$$

ρ	0.14
Λ	$0.71\ \text{GeV}^2$
ϕ_C	0.577

$$G(t) = \left(\frac{\Lambda}{\Lambda + |t|}\right)^2 , \quad \text{Proton dipole form factor}$$

$$\phi(t) = -\ln\frac{B|t|}{2} - \phi_C , \quad \text{Coulomb phase}$$

From $\frac{d\sigma}{dt}$ to $\sigma(pp)$ measurement

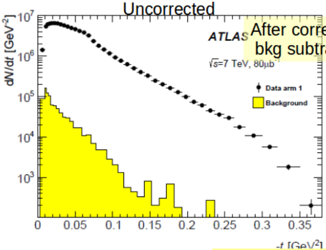

After corrections, acceptance, bkg subtraction, unfolding etc...

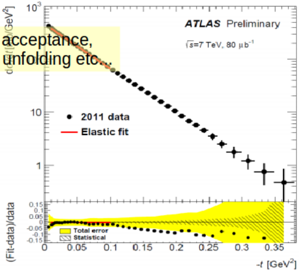

$$t = -(p\theta^*)^2$$

From the fit:

σ_{tot}=95.4 ±1.3 mb

B = 19.73 ±0.24 GeV^{-2}

$$\sigma_{el} = \frac{\sigma_{tot}^2}{B}\frac{1+\rho^2}{16\pi(\hbar c)^2}$$

σ_{el}=24.0 ±0.6 mb

By subtraction → σ_{Inel}=71.3±0.90 mb

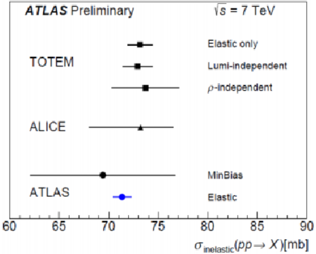

Further development (AFP)

Silicon Tracking Detectors:
- Measure position and angle
- Radiation hardness (~30 kGy/year @ 10^{34} $cm^{-2}s^{-1}$)
- → Silicon 3D detectors

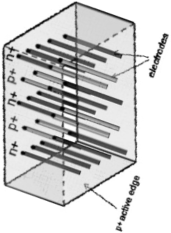

Timing detectors:
- MHz rate capability
- Trigger capability
- Quartz based Cherenkov detector + Microchannel plate PMT
- Timing resolution: σ(t)~10~20ps → σ(z) few mm

→ factor 40 of background from pileup rejection (μ=50

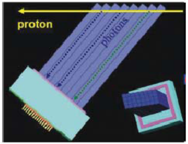

Rapidity Gaps

$\Delta\eta_F$ is defined as “largest η gap in the event”

Large $\Delta\eta_F$ sample is composed by SD + DD Events

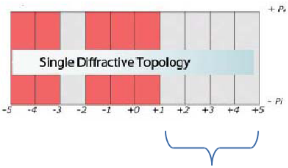

$\Delta\eta_F$=4

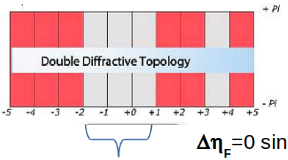

$\Delta\eta_F$=0 since Forward Rapidity gaps start at η edge

Measure differential cross section varying P_T thresholds and comparing different MC (PHOJET, Pythia 6 and Pythia 8)

$$\frac{d\sigma}{d\Delta\eta_F}$$

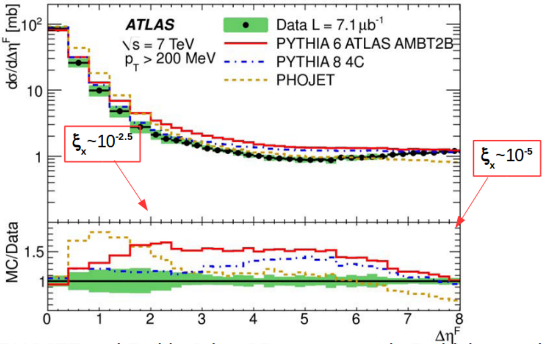

Both PHOJET and Pythia 8 (no CD component in Pythia) reproduce trend but agreement not perfect:

- PHOJET better at large $\boldsymbol{\Delta\eta_F}$ → SD and DD diffraction xsection
- Pythia better for smaller $\boldsymbol{\Delta\eta_F}$ → Sensitivity to hadronization fluctuations and MPI

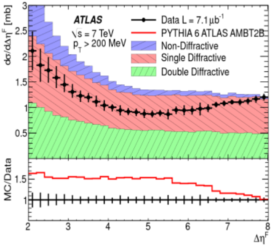

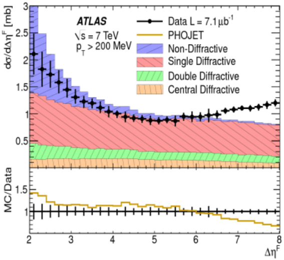

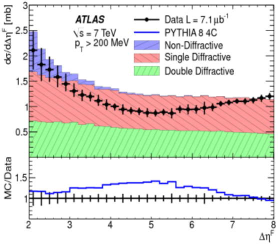

For large rapidity gaps
Plateau reproduced by both models
Raise at $\boldsymbol{\Delta\eta_F}$ >~5 not predicted by models (Triple Pomeron exchange)

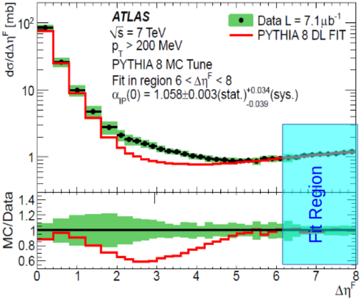

Default Pythia and Phojet $\alpha(t=0) = 1$

Increase at large $\Delta\eta_F$ is expected from the IPIPIP term in triple Regge models with a Pomeron intercept $\alpha_{IP}(t=0)>1$

→ Supercriticality of the Pomeron Regge intercept

Intercept determined by χ^2 fit for $6<\Delta\eta_F$

Low dependence on slope

$$\alpha_{I\!P}(t=0) = 1.058 \pm 0.003(\mathrm{stat})^{+0.034}_{-0.039}(\mathrm{syst})$$

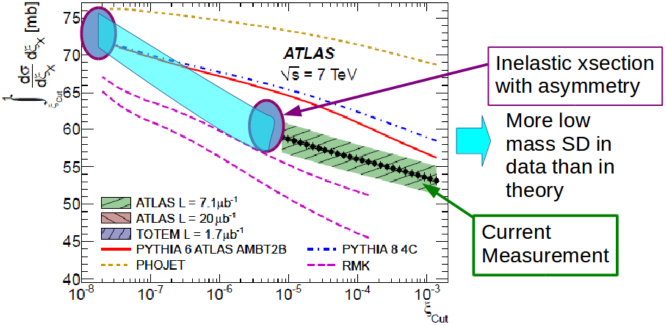

Vertical bars → all uncertainty except luminosity

Single cross section measurements performed with detectors at different η

Eur. .Phys. J. C72 (2012) 1926, arXiv1201:2808

Per aspera ad astra I

- *Handbook of Perturbative QCD* (from CTEQ Collaboration) ▸ CTEQ Handbook
- *Quantum Chromodynamics* (G. Dissertori, I.G. Knowles and M. Schmelling) Oxford University Press
- *Introduction to QCD* (P. Skands) ▸ QCD
- *Elements of QCD for hadron colliders* (G. P. Salam) ▸ QCD
- *QCD and Collider Physics* (R.K. Ellis, W.J. Stirling and B.R. Webber) Cambridge University Press
- *A QCD Primer* (G. Altarelli) ▸ arXiv:hep-ph/0204179
- *Particle Data Group 2014* (from PDF Collaboration) ▸ PDG
- *Towards Jetography* (G. P. Salam) ▸ arXiv:0906.1833
- *Quantifying the performance of jet definitions for kinematic reconstruction at the LHC* (G. P. Salam *et al.*) ▸ arXiv:0810.1304
- *Predictive Monte Carlo tools for LHC physics* (F. Maltoni) ▸ Lectures on MC
- *LHC detector papers* ▸ http://jinst.sissa.it/LHC/
- *CMS Jet Energy Scale paper* ▸ http://iopscience.iop.org/1748-0221/6/11/P11002/
- *ATLAS JES paper* ▸ http://arxiv.org/abs/1406.0076

Backup

SU(3)

$$\lambda^1 = \begin{pmatrix} 0 & 1 & 0 \\ 1 & 0 & 0 \\ 0 & 0 & 0 \end{pmatrix}, \lambda^2 = \begin{pmatrix} 0 & -i & 0 \\ i & 0 & 0 \\ 0 & 0 & 0 \end{pmatrix}, \lambda^3 = \begin{pmatrix} 1 & 0 & 0 \\ 0 & -1 & 0 \\ 0 & 0 & 0 \end{pmatrix}, \lambda^4 = \begin{pmatrix} 0 & 0 & 1 \\ 0 & 0 & 0 \\ 1 & 0 & 0 \end{pmatrix},$$

$$\lambda^5 = \begin{pmatrix} 0 & 0 & -i \\ 0 & 0 & 0 \\ i & 0 & 0 \end{pmatrix}, \lambda^6 = \begin{pmatrix} 0 & 0 & 0 \\ 0 & 0 & 1 \\ 0 & 1 & 0 \end{pmatrix}, \lambda^7 = \begin{pmatrix} 0 & 0 & 0 \\ 0 & 0 & -i \\ 0 & i & 0 \end{pmatrix}, \lambda^8 = \begin{pmatrix} \frac{1}{\sqrt{3}} & 0 & 0 \\ 0 & \frac{1}{\sqrt{3}} & 0 \\ 0 & 0 & \frac{-2}{\sqrt{3}} \end{pmatrix}.$$

One convention is: $T^A \equiv= \frac{1}{2}\lambda^A$
Structure constant:
$[T^a, T^b] = iC^{abc}T^c$

$$\begin{aligned} C^{123} &= 1 \\ c^{458} &= C^{678} = \sqrt{3}/2 \\ C^{147} &= C^{165} = C^{246} = C^{345} = C^{376} = C^{257} = 1/2 \end{aligned}$$

all others are null

$$Tr(T^a T^b) = \frac{1}{2}\delta_{ab}$$

MC@NLO

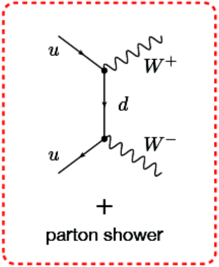

HERWIG

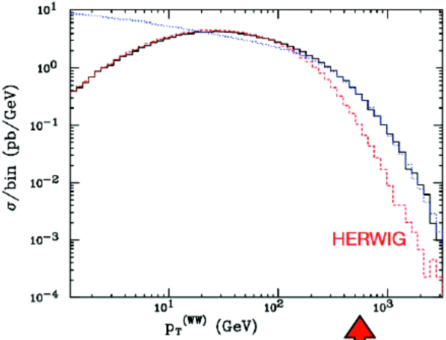

Herwig too soft in the high-p_t region

169

MC@NLO

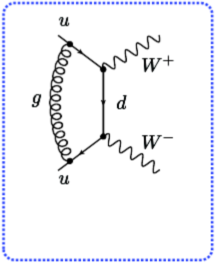

NLO

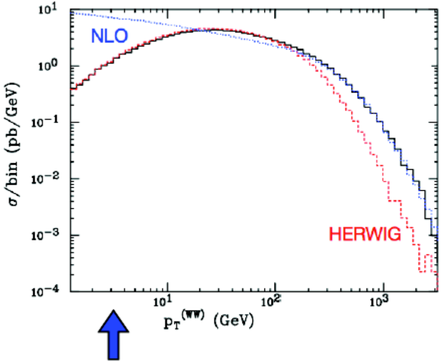

NLO divergent
in the soft region

MC@NLO

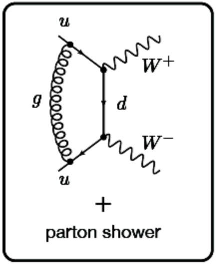

MC@NLO

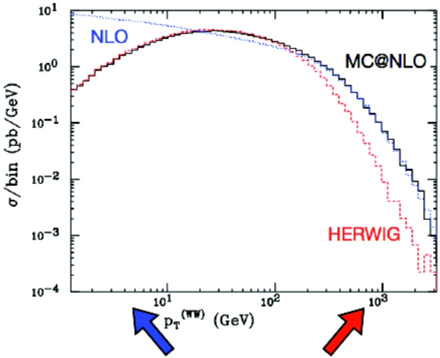

MC@NLO correctly interpolates between the two regimes

Jet Algorihms in past and present experiments

Algorithm	Type	IRC safe?	Ref.	Notes
inclusive k_t	$SR_{p=1}$	OK	[27, 28, 29]	also has exclusive variant
Cambridge/Aachen	$SR_{p=0}$	OK	[30, 31]	
anti-k_t	$SR_{p=-1}$	OK	[33]	
SISCone	SC-SM	OK	[40]	multipass, with optional cut on stable cone p_t
CDF JetClu	IC_r-SM	IR_{2+1}	[36]	
CDF MidPoint cone	IC_{mp}-SM	IR_{3+1}	[21]	
CDF MidPoint searchcone	$IC_{se,mp}$-SM	IR_{2+1}	[51]	
DØ Run II cone	IC_{mp}-SM	IR_{3+1}	[21]	no seed threshold, but cut on cone p_t
ATLAS Cone	IC-SM	IR_{2+1}	[16]	
PxCone	IC_{mp}-SD	IR_{3+1}	[38]	no seed threshold, but cut on cone p_t,
CMS Iterative Cone	IC-PR	$Coll_{3+1}$	[17]	
PyCell/CellJet (from Pythia)	FC-PR	$Coll_{3+1}$	[100]	
GetJet (from ISAJET)	FC-PR	$Coll_{3+1}$		

Jet Clustering Algorithm Optimization

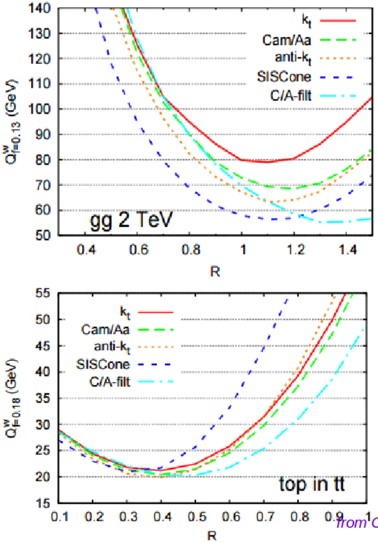

Use larger R (1.0) for jets from heavy resonances and jets from gluons rather than quark

Different R_{Opt} for different jet reconstruction algoritms but common trend is evident.

from Cacciari, Rojo and Salam arXiv:0810.1304

Noise in ATLAS Calorimeters

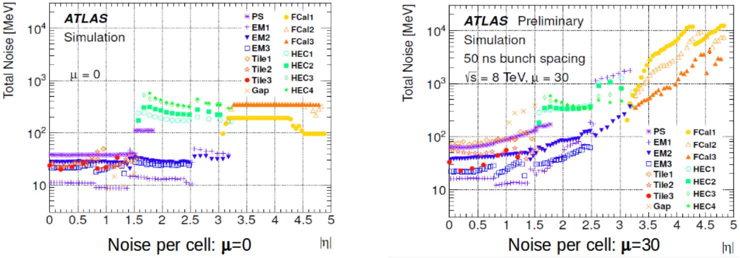

from ATLAS-CONF-2014-018 and paper in preparation (EPJC)

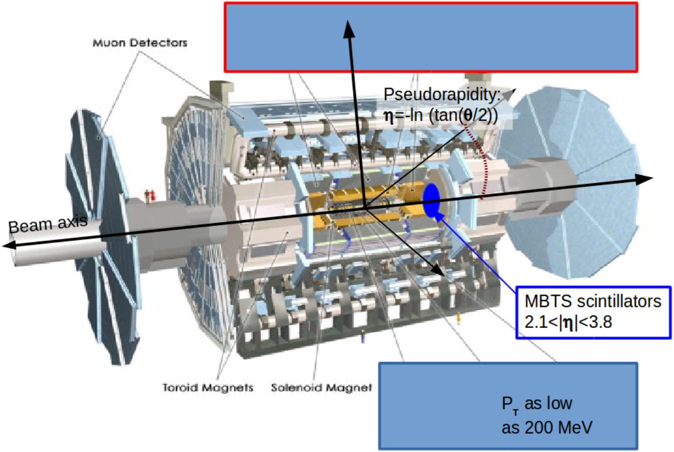
Muon Detectors
Pseudorapidity:
η=-ln (tan(θ/2))
Beam axis
MBTS scintillators
2.1<|η|<3.8
Toroid Magnets
Solenoid Magnet
P_T as low
as 200 MeV

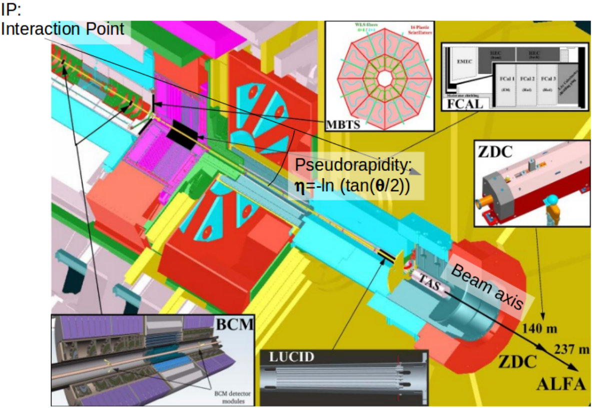
IP:
Interaction Point
MBTS
FCAL
ZDC
Pseudorapidity:
η=-ln (tan(θ/2))
Beam axis
TAS
140 m
237 m
ZDC
ALFA
BCM
LUCID
BCM detector modules

From G. Wolshin EPL **95** 61001 (2011)

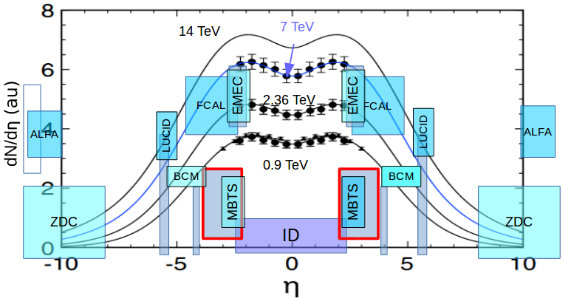

Detector	η coverage
ID (Pix + SCT)	|η|<2.5
ID (TRT)	|η|<2.0
MBTS	2.08<|η|<3.75
Calo: EMEC	2.5<|η|<3.2
Calo: FCal	3.1<|η|<4.9

Detector	η coverage
BCM	|η|=4.2
LUCID	5.6<|η|<6.0
ZDC	|η|>8.3
ALFA	10.6<|η|<13.5